Published in final edited form as:
Gastroenterology. 2007 May ; 132(5): 1834–1851. doi:10.1053/j.gastro.2007.03.038.

The Lysophosphatidic Acid Type 2 Receptor Is Required for Protection Against Radiation-Induced Intestinal Injury

Wenlin Deng[*,‡], **E Shuyu**[*], **Ryoko Tsukahara**[*], **William J. Valentine**[*], **Gangadhar Durgam**[§], **Veeresa Gududuru**[‡,§], **Louisa Balazs**[‖], **Venkatraman Manickam**[¶], **Marcello Arsura**[¶], **Lester Vanmiddlesworth**[*], **Leonard R. Johnson**[*], **Abby L. Parrill**[#], **Duane D. Miller**[§], and **Gabor Tigyi**[*,#]

[*]Department of Physiology, University of Tennessee Health Sciences Center, Memphis

[§]Department of Pharmaceutical Science, University of Tennessee Health Sciences Center, Memphis

[‖]Department of Pathology, University of Tennessee Health Sciences Center, Memphis

[¶]Department of Pharmacology, University of Tennessee Health Sciences Center, Memphis

[‡]RxBio Inc, Memphis

[#]Department of Chemistry and Computational Research on Materials Institute, University of Memphis, Memphis, Tennessee

Abstract

Background & Aims—We recently identified lysophosphatidic acid (LPA) as a potent antiapoptotic agent for the intestinal epithelium. The objective of the present study was to evaluate the effect of octadecenyl thiophosphate (OTP), a novel rationally designed, metabolically stabilized LPA mimic, on radiation-induced apoptosis of intestinal epithelial cells in vitro and in vivo

Methods—The receptors and signaling pathways activated by OTP were examined in IEC-6 and RH7777 cell lines and wild-type and LPA_1 and LPA_2 knockout mice exposed to different apoptotic stimuli

Results—OTP was more efficacious than LPA in reducing gamma irradiation–, camptothecin-, or tumor necrosis factor α/cycloheximide–induced apoptosis and caspase-3-8, and caspase-9 activity in the IEC-6 cell line. In RH7777 cells lacking LPA receptors, OTP selectively protected LPA_2 but not LPA_1 and LPA_3 transfectants. In C57BL/6 and LPA_1 knockout mice exposed to 15 Gy gamma irradiation, orally applied OTP reduced the number of apoptotic bodies and activated caspase-3–positive cells but was ineffective in LPA_2 knockout mice. OTP, with higher efficacy than LPA, enhanced intestinal crypt survival in C57BL/6 mice but was without any effect in LPA_2 knockout mice. Intraperitoneally administered OTP reduced death caused by lethal dose $(LD)_{100/30}$ radiation by 50%.

Conclusions—Our data indicate that OTP is a highly effective antiapoptotic agent that engages similar prosurvival pathways to LPA through the LPA_2 receptor subtype.

Address requests for reprints to: Gabor Tigyi, MD, PhD, Department of Physiology, University of Tennessee Health Sciences Center, 894 Union Avenue, Memphis, Tennessee 38163. gtigyi@physio1.utmem.edu; fax: (901) 448-7126.
W.D. and S.E. contributed equally to this work.

The stem cells of the intestinal mucosa represent one of the most radiation-vulnerable cell types in the mammalian body.1 Whereas free radical scavengers can ameliorate the central nervous system syndrome and the widely used bone marrow transplantation can effectively treat the hematopoietic syndrome caused by exposure to lethal doses of radiation, effectively treating the gastrointestinal syndrome due to radiation-induced apoptosis of the intestinal stem cells is more difficult.

Lysophosphatidic acid (1-radyl-2-hydroxy-*sn*-glycero-3-phosphate; LPA) is a growth factor–like lipid mediator with antiapoptotic actions elicited through a set of G protein–coupled receptors.2,3 At least 5 LPA G protein–coupled receptors have been identified so far.4 The LPA_1, LPA_2, and LPA_3 receptors are encoded by the endothelial differentiation gene (EDG) family and share approximately 60% identity with each other.2,4 LPA_4 and LPA_5 are distantly related to the EDG family, share only 20%–24% amino acid identity with the EDG family, and functionally are less well characterized.5–7 The mouse intestine predominantly expresses the LPA_1 and LPA_2 receptor subtypes.8,9 Each individual LPA receptor has its distinct coupling pattern to G proteins. LPA_1 couples to G_i, G_q, and $G_{12/13}$; LPA_2 couples to G_i, G_q, and $G_{12/13}$; and LPA_3 couples to only G_i and G_q, not $G_{12/13}$.10 These G proteins share many downstream signaling pathways that act in a cooperative manner.11 The activation of the phosphoinositide 3-kinase (PI3K)-AKT and MEK-ERK1/2 prosurvival pathways has been well delineated in mediating LPA-initiated antiapoptotic activity.12–14 LPA activates AKT, which in turn phosphorylates BAD and procaspase 9, leading to inhibition of apoptosis.15 LPA-induced activation of mitogen-activated protein kinase/extracellular signal–regulated kinase kinase (MEK)/extracellular signal–regulated kinase (ERK) 1/2 signaling can also activate BAD phosphorylation and attenuate caspase-9.16 LPA has been shown to activate nuclear factor κB, which regulates important prosurvival genes.16,17 A specific cellular response, including the antiapoptotic effect of LPA, might be mediated through a single LPA receptor or a combination of multiple receptor subtypes, which appear to be coexpressed in most cell types.18 Because LPA receptors are ubiquitously expressed and because of the overlapping coupling patterns to G proteins, elucidating the biological responses mediated by each individual receptor requires targeted gene knockout (KO) animal models. LPA_1, LPA_2, and LPA_1/LPA_2 double KO animals have been generated and show minimal phenotypes.19–21 At the present time, it remains unknown which LPA receptor(s) is required for its antiapoptotic effect in the different organs.

LPA in the gastrointestinal tract derived from foods such as soybean,22–25 metabolism of phospholipids by phospholipases,26 or activated platelets under pathological conditions.27 High levels of phospholipids have been detected in the colonic mucosa of patients with inflammatory bowel disease, and LPA significantly reduces the degree of inflammation and necrosis in a rat model of colitis.27 LPA has been shown to stimulate restitution of intestinal epithelia via pertussis toxin (PTX)-sensitive mechanisms.28 LPA_2 receptors play an important attenuating role in bacterial toxin–induced secretory diarrhea via PDZ domain–mediated protein-protein interactions, inhibiting the activation of the CFTR Cl^- channel.8 Therefore, the food-derived LPA in the lumen and its receptors on the epithelium suggest a physiologic role for LPA in maintaining gastrointestinal integrity that can be explored for therapeutic intervention.

Apoptosis in the intestinal epithelium is the primary pathologic factor that leads to chemotherapy- or radiation-induced gastrointestinal damage.1,29,30 We formulated a hypothesis that LPA can be used for the protection of the mucosa from iatrogenic traumas (radiation injury in particular); if so, it could serve as a template for prosurvival drugs against radiation injury. This hypothesis is based on several lines of our work reported over the past few years. We showed that LPA protected intestinal epithelia against irradiation-

induced apoptosis both in vitro and in vivo,12 also showed in vitro that LPA achieved its antiapoptotic effects through the PTX-sensitive activation of the MEK-ERK1/2 and PI3K–AKT prosurvival pathways,13 and established that the antiapoptotic effect, unlike the mitogenic and motogenic effects of LPA, did not require the transregulation of several tyrosine kinase receptors.31 However, LPA is not an optimal drug candidate. Exogenous LPA is rapidly metabolized in the gastrointestinal tract. Because complex lipids, including phospholipids, are broken down to nonpolar intermediates that traverse the plasma membrane, the action of LPA is terminated by phospholipase- and lipase-mediated deacylation or (lipid) phosphatase-mediated dephosphorylation. While this mechanism rapidly renders LPA inactive, it also limits the effect of LPA on the receptors present on the luminal surface of the epithelium. LPA consists of a glycerol backbone with a hydroxyl group, a phosphate group, and a fatty acid or fatty alcohol chain. We have developed and experimentally validated computational models of the EDG family of LPA receptors32–38 and established the absolute requirement for a negatively charged headgroup and the aliphatic tail but not for the glycerol backbone.34,39,40 Therefore, we hypothesized that long-chain fatty alcohol thiophosphates mimic LPA at the EDG family receptors and at the same time are metabolically stabilized against phospholipase cleavage, which requires a glycerol backbone. Furthermore, thiophosphates tend to be poor substrates of lipid phosphatases and render them resistant to breakdown. These observations led us to explore the pharmacologic and biologic properties of octadecenyl thiophosphate (OTP) as an orally bioavailable, metabolically stabilized, nonabsorbing LPA mimic with radioprotective action in the gut.

The present study set multiple objectives. First, we explored the pharmacologic properties of OTP by using computational and pharmacologic approaches and determined its resistance to lipase and lipid phosphatase cleavage. Next, we compared the antiapoptotic effect of OTP with that of LPA in IEC-6 cells in vitro. Third, using a receptor add-back, we examined which LPA receptor subtypes mediate survival signals to prevent radiation-induced apoptosis. Fourth, we examined whether orally applied OTP reduces radiation-induced apoptosis and caspase-3 activation and increases crypt survival in clonogenic assays conducted in C57BL/6 mice exposed to 15 Gy gamma irradiation. We also evaluated the OTP- and LPA-induced activation of those prosurvival signaling pathways in vivo that we had previously established in vitro. Finally, we tested whether intraperitoneal administration of OTP prevents death caused by $LD_{100/30}$ gamma irradiation. We found that OTP mitigated radiation-induced death, protected intestinal epithelial cells from apoptosis in vitro and in vivo, and was significantly more effective compared with LPA. Both LPA and OTP reduced apoptosis and caspase-3 activation and increased crypt survival in wild-type and LPA_1 KO mice; however, both were ineffective in LPA_2 KO mice. Together, these data suggest that OTP is a highly effective intestinal radioprotective agent that targets LPA_2 as a prosurvival receptor.

Materials and Methods

Reagents

LPA (oleoyl) was purchased from Avanti Polar Lipids (Alabaster, AL). LPA and OTP (synthesized as described by Durgam et al40) were applied to cells complexed with fatty acid–free bovine serum albumin (BSA; Sigma Chemical Co, St Louis, MO) as previously described.39 Camptothecin and cycloheximide (CHX) were purchased from Sigma Chemical Co. Recombinant rat tumor necrosis factor (TNF)-α was purchased from BD PharMingen (San Diego, CA). PD98059 was purchased from Calbiochem (San Diego, CA). PTX and Ac-DEVD-pNA and Ac-LEHD-pNA colorimetric and Ac-IETD-AFC fluorescent caspase substrates were from Biomol Laboratories, Inc (Plymouth Meeting, PA). The following antibodies and sources were used: rabbit anti–caspase-3 (Santa Cruz

Biotechnology, Inc, Santa Cruz, CA), rabbit anti-active caspase-3 (Abcam, Inc, Cambridge, MA), mouse monoclonal anti-JNK1 (BD PharMingen), mouse monoclonal anti-phospho (Thr^{183}/Tyr^{185})-JNK, rabbit anti-ERK1/2, rabbit anti-phospho-(Tyr^{202}/Tyr^{204}) ERK1/2, rabbit anti-AKT, rabbit anti-phospho-(Ser^{473})-AKT, rabbit anti–Bcl-2, monoclonal mouse anti–Bcl-X_L (Cell Signaling, Inc, Beverly, MA), monoclonal mouse anti–phospho-(Thr^{180}/Tyr^{182})-P38 (Promega, Madison, WI), and mouse monoclonal anti-actin (Calbiochem). Horseradish peroxidase–conjugated anti-rabbit and anti-mouse secondary antibody used for Western blotting was purchased from Sigma Chemical Co. Fluorescein isothiocyanate–labeled goat anti-rabbit immunoglobulin G was purchased from Molecular Probes (Eugene, OR). Normal goat serum and Vectashield Mounting Medium with DAPI were purchased from Vector Laboratories, Inc (Burlingame, CA).

Computational Modeling

The detailed methods used to develop computational models of LPA_1, LPA_2, and LPA_3 have been reported previously.[33,34,36] Briefly, our validated model of the S1P1 receptor[32,33,37] was used as a template for generating LPA receptor models. Homology model development was performed using the automated algorithm implemented in the MOE software program.[41] The best model was geometry optimized using the MMFF9442 force field to a root mean square gradient of 0.1 kcal/mol Å. The individual receptor models were used in docking studies with OTP bearing a total charge of −2. Docking calculations were performed using Autodock 3.0 software[43] with default values for all parameters except the number of runs (10), energy evaluations (9.0×10^{10}), generations (60,000), and local search iterations (3000). The complex chosen as the best geometry from each docking calculation was that with the lowest final docked energy value. Results are described using a numbering system that facilitates comparisons among homologous positions in G protein–coupled receptors as described by Ballesteros and Weinstein.[44] In this system, each amino acid in the transmembrane domain is given a number in the format X.YY where X indicates the number of the transmembrane helix where the amino acid is found and YY indicates the position relative to the most conserved amino acid in that helix at reference position 50.

Radiolabeling of OTP

Tritiated OTP was synthesized in our laboratory as shown in Figure 1*D*. Pyridinium chlorochromate–mediated oxidation of oleyl alcohol gave oleyl aldehyde (2), which was subjected to reduction with NaB_3H_4 to form the tritiated oleyl alcohol (3). Alcohol 3 was phosphorylated as reported earlier[40] to give protected oleyl thiophosphate ester (4). Treatment of 4 with methanolic KOH, followed by acidification, yielded [^{3}H]-OTP. The specific activity of the product was 10.8 mCi/mmol.

Determining OTP Absorption From the Gut

To determine oral absorption of OTP, female 8- to 10-week-old C57BL/6 mice (average body wt, 20 g) were used. Mice were maintained on a 12-hour light/12-hour dark cycle and fed standard laboratory mouse chow and water ad libitum. Conscious mice were administered through oral gavage 1.5 mg/kg OTP in 1 mmol/L BSA in phosphate-buffered saline (PBS) including 10^6 dpm OTP. Groups of 4 mice were killed after 60, 90, and 180 minutes, and blood samples were collected through cardiac puncture using 0.2% EDTA anticoagulant. Ten-microliter whole-blood samples from each mouse were mixed with Ecolume (Packard, Boston, MA) liquid scintillation cocktail and counted after 24 hours of equilibration in a liquid scintillation counter.

Assaying OTP Metabolism by Pancreatic Lipase and Lipid Phosphate Phosphatase 1

To determine the enzymatic stability of OTP by phospholipases, [^{3}H]-OTP (5.2×10^6 dpm) mixed with 0.03 mmol/L cold OTP was subjected to enzymatic hydrolysis for 24 hours by using bovine pancreatic lipase (Sigma Chemical Co) followed by thin-layer chromatography (TLC) separation of the products using a previously established protocol.45 Lipid phosphate phosphatase (LPP) was obtained from mouse embryonic fibroblasts derived from mice with transgenic overexpression of the enzyme.46 Membrane fractions (300 μg/reaction) prepared by centrifugation at $10^4 \times g$ from transgenic LPP1 fibroblasts were added to [^{3}H]-OTP (1.5×10^6 dpm) mixed with 8 μmole cold OTP and subjected to LPP1 hydrolysis for 8 hours using a previously established protocol.46 The reaction mixture was dried in vacuo, and the residue was acidified with 100 μL 1N HCl and extracted 4 times with 0.5 mL ethyl acetate. The extracts were combined, and the solvent was evaporated. The extracted reaction products were taken up in 2 mL ethyl acetate, and a 20-μL aliquot was applied to TLC using methanol/ether solvent (2:98 vol/vol) as described.45

Cell Culture and Induction of Apoptosis In Vitro

IEC-6 and the rat hepatoma RH7777 cells were obtained from the American Type Culture Collection (Manassas, VA). IEC-6 cells were grown in Dulbecco's modified Eagle medium supplemented with 10% fetal bovine serum, insulin (10 μg/mL), and gentamicin sulfate (50 μg/mL) at 37°C in a humidified 90% air/10% co_2 atmosphere. RH7777 cells, stably expressing LPA_2 receptors, were provided by Dr Fumikazu Okajima (Gunma University, Maebashi City, Japan). RH7777 cells stably expressing LPA_1 or LPA_3 receptors were generated by our group and characterized elsewhere.47 Wild-type and stably transfected RH7777 cells were grown in Dulbecco's modified Eagle medium with 10% fetal bovine serum and 2 mmol/L glutamine containing 250 μg/mL G418 for the stable transfectants. Apoptosis in IEC-6 cells was induced by exposing them to 20 μmol/L camptothecin or a 25-Gy Cs^{137} source gamma irradiation (Mark I model 25 Gamma Irradiator; J. L. Shepherd & Associates, San Fernando, CA) at a rate of 4.80 Gy/min. DNA fragmentation and caspase-3 activity were measured 6 hours after camptothecin treatment or 18 hours postirradiation. Apoptosis in RH7777 cells was induced by 20 ng/mL TNF-α plus 10 μg/mL CHX and evaluated 6 hours later.

Pharmacologic Characterization of OTP

The ligand properties of OTP were evaluated using RH7777 cells stably transfected with each LPA receptor of the EDG family exactly as described in our previous report.40 RH7777 cells lack endogenous Ca^{2+} responses to LPA applied as high as 30 μmol/L, the highest concentration tested, but acquire these responses upon transfection of any of the LPA receptors.39,40,47 Briefly, RH7777 cells stably expressing human LPA_1, LPA_2, or LPA_3 were loaded with Fura-2 AM (Invitrogen, Carlsbad, CA). Changes in intracellular Ca^{2+} concentration were monitored by measuring the ratio of emitted light intensity at 520 nm in response to excitation by 340-nm and 380-nm wavelength lights, respectively, using a FlexStation II robotic fluorescence plate reader (Molecular Devices, Sunnyvale, CA). Responses were monitored for 80–120 seconds. Ca^{2+} transients were quantified automatically by calculating the difference between maximum and baseline ratio values for each sample run in triplicate.

Reverse-Transcription Polymerase Chain Reaction

RNA was extracted using TRIzol (Invitrogen) from wild-type and KO mice using four 0.5-cm segments spaced equally along the jejunum. The following gene-specific primers were used: LPA_1: forward 5′-TCTGAAGACTGTG GTCATTGTGC-3′, reverse 5′-GCCATTAGGGTTCTCGT-TGC-3′; LPA_2: forward 5′-CACTCCTGGCACT GCCTCT-

GTG-3′, reverse 5′-TAC GGC GCA TCT CAG CGT CTC G-3′; LPA_3: forward 5′-ACACATGTCAATCATGAGGAT-3′, reverse 5′-GAA GACGGTGACTGTCTTAGG-3′; LPA_4: forward 5′-GAAGGCTTCTCCAAACGT GTCTG-3′, reverse 5′-C CTTG TGCCTTGCAACTCTGAA-3′; LPA_5: forward 5′-CTGATGCTC ATCAACGTGGACC-3′, reverse 5′-TAGGGCACGAAGCACAGCAG-3′; β-actin: forward 5′-GACAACG GCTCCGGCATGTG-3′, reverse 5′-TTGAGACCT TCAACACCCCAGCA-3′. Reverse-transcription polymerase chain reaction was performed using the Superscript III kit (Invitrogen), and a total of 31 cycles were performed; the products were applied in full to agarose gels and stained with ethidium bromide.

Evaluating Apoptosis by DNA Fragmentation and Caspase Activity

DNA fragmentation was measured by enzyme-linked immunosorbent assay following the procedure provided with the Cell Death Detection Kit from Roche (Indianapolis, IN) as described previously12,13 and was expressed as absorbance units (at 405 nm) per microgram protein per minute. Caspase-3 and caspase-9 activity in IEC-6 cells were measured by enzyme-linked immunosorbent assay by using the specific Ac-DEVD-pNA chromogenic substrate for caspase-3 and Ac-LEHD-pNA for caspase-9 as described previously.12,13 Small intestine samples were washed thoroughly with PBS, scraped off the muscle layer, mixed with lysis buffer, homogenized, and centrifuged. The supernatants were collected for evaluating caspase-3 activity as described previously. Caspase-3 and caspase-9 activity were expressed as picomole pNA cleaved per minute per microgram protein. Caspase-8 activity was measured by using the specific Ac-IETD-AFC fluorescent substrate. Each reaction contained 20 μL cytosolic proteins, 70 μL assay buffer (50 mmol/L HEPES [pH 7.4], 100 mmol/L NaCl, 10 mmol/L dithiothreitol, 1 mmol/L EDTA, and 0.1% [vol/vol] 3-[(3-cholamidopropyl)-dimethylammonio]-1-propanesulfonate detergent), and 10 μL of 2 mmol/L Ac-IETD-AFC dissolved in assay buffer. The enzymatic reaction was performed in 96-well plates at 37°C and monitored using a FlexStation II microplate reader (Molecular Devices) at 37°C with fluorescence excitation at 405 nm and emission at 505 nm. Protein concentration was measured by using the Bradford protein assay kit (Bio-Rad, Hercules, CA), and caspase-8 activity was expressed as arbitrary fluorescence units per milligram per minute.

Western Blotting

Caspase-3 was measured in IEC-6 cells or intestinal epithelial lysates prepared for caspase-3 activity as described in our previous reports.12,13 ERK1/2 and AKT were measured in total cellular protein lysates by using a previously described procedure.13 Briefly, IEC-6 cells were lysed in 62.5 mmol/L Tris-HCl (pH 6.8), 2% sodium dodecyl sulfate, 25% glycerol, 1 mmol/L NaF, 1 mmol/L orthovanadate, and protease inhibitor cocktail (Sigma Chemical Co). The lysates were cleared by centrifugation ($10^4 \times g$) for 15 minutes at 4°C, and supernatants were collected. Protein concentrations were determined using the BCA Reagent Kit (Pierce Biotechnology, Inc, Rockford, IL). For ERK1/2, AKT, p38, and JNK, 10 μg, 40 μg, 20 μg, and 50 μg, respectively, of the cell lysate was fractionated by sodium dodecyl sulfate/polyacrylamide gel electrophoresis and transferred to polyvinylidene difluoride membranes, blocked with 5% nonfat milk, and incubated with various primary antibodies. Blots reacted with the appropriate horseradish peroxidase–conjugated secondary antibodies and developed using the SuperSignal chemiluminescence reagent (Pierce Biotechnology, Inc).

For Western blotting of Bcl-X_L and Bcl-2, IEC-6 cells were harvested and washed with PBS twice and then resuspended with 100–200 μL ice-cold lysis buffer (20 mmol/L Tris [pH 7.5], 150 mmol/L NaCl, 1 mmol/L EDTA, 1 mmol/L ethylene glycol-bis(β-aminoethyl ether)-*N,N,N′,N′*-tetraacetic acid, 1% Triton X-100, protease inhibitor, and phosphatase

inhibitor cocktails [Sigma Chemical Co]). Cells were sonicated 3 times for 3 seconds each, and the lysate was centrifuged at 16,100*g* for 20 minutes at 4°C. The supernatants were collected. Protein concentration was measured by using the BCA Protein Assay Kit (Pierce Biotechnology, Inc).

Animal Treatment and Irradiation

The whole-body irradiation protocol was reviewed and approved by the University of Tennessee Health Science Center Animal Care and Use Committee. Eight-to 10-week-old C57BL/6 mice were purchased from Harlan (Indianapolis, IN) and maintained on a 12-hour light/12-hour dark cycle and fed standard laboratory mouse chow and water ad libitum. LPA_1 and LPA_2 KO mice generously provided by Dr Jerold Chun (Scripps Research Institute, La Jolla, CA) were bred in house and used between the ages of 8 and 12 weeks. Mice were fasted overnight before whole-body gamma irradiation (Cs^{137} source at a rate of 4.80 Gy/min). LPA or OTP was administered by oral gavage 2 hours before irradiation. Mice were killed either 4 hours after irradiation by isoflurane inhalation for analysis of apoptosis or 4 days later for the clonogenic assay. Four segments of the jejunum and the ileum were fixed in 10% neutralized formaldehyde (pH 7.4) buffer and processed for histologic evaluation. Mice used in the clonogenic regeneration assay received bromodeoxyuridine (BrdU; 120 mg/kg) and 5-fluoro-2′-deoxyuridine (5FdU; 12 mg/kg) intraperitoneally 2 hours before death to label the S-phase regenerating cells in intestine.

Testing the Acute Toxicology of OTP

Female 8-week-old C57BL/6 mice (average body wt, 20 g) were maintained on a 12-hour light/12-hour dark cycle and fed standard laboratory mouse chow and water ad libitum. Mice were randomly grouped into groups of 5 and weighed daily before oral gavage of 3, 10, and 30 mg/kg OTP dissolved in 1 mmol/L BSA in PBS. Mice were observed for 1 hour after OTP treatment, and any abnormal behavior and change in regular motor activity was recorded. Weights were monitored for 5 consecutive days after OTP treatment.

Assessing Apoptosis and Crypt Survival in Intestine

Paraffin cross sections were cut perpendicular to the long axis of the small intestine and stained with H&E or immunostained with a monoclonal anti-BrdU antibody. Epithelial cell apoptosis and crypt survival were analyzed in 2 sections per segment as previously described.12 To detect apoptosis, a minimum of 100 half crypt-villus units from each experimental group were scored and the number of apoptotic bodies per intestinal circumference was counted. For the clonogenic assay, the number of surviving crypts per jejunal circumference was counted in the sections from the different segments. A surviving crypt was defined as a regenerative crypt that contained a cluster of 10 or more H&E-stained cells. The viability of surviving crypts was confirmed by positive immunostaining for BrdU or incorporation of 5FdU into 5 or more crypt cells.

Immunohistologic Staining

To identify the BrdU-labeled S-phase cells in the crypts, we used a staining protocol described in our previous report.48 For activated caspase-3 staining, formalin-fixed, paraffin-embedded tissue sections were used with heat-mediated antigen retrieval for 15 minutes. After three 5-minute washes in Tris-buffered saline (25 mmol/L Tris, 150 mmol/L NaCl, pH 7.6), slides were blocked with 10% normal goat serum in Tris-buffered saline/0.1% Tween-20 for 2 hours at room temperature. Rabbit anti-active caspase-3 antibody was diluted 1:50 in 1% BSA/Tris-buffered saline/0.1% Tween-20 and incubated at 4°C overnight. Fluorescein isothiocyanate–labeled goat anti-rabbit immunoglobulin G was applied for 2 hours after washes, and the slides were mounted with Vectashield Mounting

Medium with DAPI (Vector Laboratories) and visualized by a Nikon Eclipse 80i fluorescence microscope (Dallas, TX). At least 100 crypt-villus units per animal were counted for the presence of activated caspase-3–positive cells.

Immunohistochemical staining for Bcl-X_L and Bcl-2 was performed using 5-μm-thick sections cut from formalin-fixed, paraffin-embedded blocks of jejunum and ileum taken 4 hours after irradiation from a total of 6 mice. Upon antigen unmasking, immunostaining with primary antibody (1:25 dilution) was performed using the rabbit Vectastain ABC Elite Kit (Vector Laboratories) following the manufacturer's instructions. Vector 3,3′-diaminobenzidine peroxidase substrate (Vector Laboratories) was used for color development. Stained sections were then dehydrated and counterstained with Vector Hematoxylin QS (Vector Laboratories), and immunoreactivity was assessed by at least 2 investigators.

Monitoring the Radiation-Mitigating Effect of OTP on Survival

Conscious 8-week-old female mice were injected with 0.5 mg/kg OTP or vehicle (2% dimethyl sulfoxide/ PBS) 30 minutes before irradiation with 9 Gy ($LD_{100/30}$) of gamma irradiation. Each group consisted of 18 mice, which provided 90% statistical power based on a Fisher exact test with a one-sided 5% significance level. The primary end point was survival to day 30. The secondary end point was the mean survival time of decedents.

Statistical Analysis

Data are expressed as means ± SD or SEM. Each in vitro experiment was repeated at least 3 times. For animal studies, each experimental group consisted of at least 6 mice; a minimum of 8 KO mice was used per group. Student *t* test was used for comparing control and treatment groups. A *P* value of <.05 was considered significant.

Results

Molecular Modeling and Pharmacologic Characterization of OTP

Complexes of OTP with the LPA receptor models are shown in Figure 1*B*. The LPA_1 complex showed a strong ionic interaction between the thiophosphate group and R3.28 (2.0 Å P-O:H-N distance). No interaction occurred involving Q3.29, a residue required for LPA binding and LPA-induced LPA_1 receptor activation.33 Similar to the LPA_1 complex, the LPA_3 complex failed to show a strong hydrogen bonding interaction with Q3.29 due to the unfavorably nonlinear angle49 formed by the amide N-H and the hydrogen bond acceptor (112°). However, a greater number of strong ionic interactions were observed in the LPA_3 complex involving not only R3.28 but also K7.35 (2.2 Å P-O:H-N and 2.4 Å P-S:H-N distances, respectively). In contrast to our previous studies demonstrating a role for R5.38 in LPA-induced LPA_3 activation,36 OTP failed to interact with R5.38. The failure of OTP to interact with residues known to be required for LPA-induced activation of LPA_1 and LPA_3 is consistent with the observation of only partial agonism at these receptors (Figure 1*C*). OTP showed both strong ionic interaction with R3.28 (1.6 Å P-O:H-N distance) and moderate hydrogen bonding interaction with Q3.29 (142°). This hydrogen bonding angle was within the most highly populated cluster of angles observed in crystal structures.49 The LPA_2 receptor lacks cationic amino acid residues at the top of TM7, so these 2 interactions comprise the required headgroup interactions for full agonism.

LPA and OTP activate LPA receptors stably expressed in RH7777 cells, providing a simple assay platform to study the pharmacologic properties of these receptors as described in many previous reports.39,40,47,50 OTP was compared in wild-type, LPA_1, LPA_2, and LPA_3 transfected RH7777 cells using Ca^{2+} mobilization as a measure of receptor activation

(Figure 1*C*). OTP was inactive in wild-type RH7777 cells up to 30 μmol/L, the highest concentration tested (data not shown). However, it activated all 3 EDG family LPA receptors with varying potency and efficacy. OTP was always less potent than oleoyl LPA at all 3 receptors and was less efficacious at LPA_1 and LPA_3 receptors. At the LPA_2 receptor subtype, OTP was a full agonist and showed an apparent median effective concentration of 90 nmol/L compared with 1 nmol/L for oleoyl LPA. Thus, OTP is a less efficacious full agonist of the LPA_2 receptor subtype.

Metabolic Resistance of OTP to Pancreatic Lipase and LPP1

The 2 major pathways of LPA breakdown include (phospho)lipase-mediated deacylation and lipid phosphate phosphatase–mediated dephosphorylation.51 To determine the enzymatic stability of OTP by pancreatic lipase and LPP1, we synthesized [^{3}H]-OTP for monitoring the enzymatic hydrolysis followed by TLC separation of the products using previously established protocols.45,46 TLC analysis of the pancreatic lipase–mediated hydrolysis of [^{3}H]-OTP for up to 24 hours showed neither the breakdown nor formation of the expected [^{3}H]-oleyl alcohol (data not shown). In contrast, LPA was fully metabolized under these conditions. The lack of cleavage is consistent with the requirement for the glycerol backbone that is absent in the OTP structure. LPP1 cleavage of [^{3}H]-OTP for up to 8 hours showed no detectable dephosphorylation, indicating that the thiophosphate moiety is considerably more resistant to cleavage by this enzyme than the phosphate moiety present in LPA.

Absorption of Orally Applied OTP Into the Blood

The absorption of orally administered OTP into the bloodstream was determined by injecting 10^6 dpm [^{3}H]-OTP tracer mixed with cold OTP to yield 1.5 mg/kg into the stomach. Blood samples collected 60, 90, and 180 minutes later showed that as little as 0.67% ± 0.15%, 0.61% ± 0.2%, and 0.45% ± 0.15% of the applied radioactivity appeared in the blood compartment. Assuming that all of it was nonmetabolized OTP, this would yield a maximal blood concentration of 180 nmol/L, which could activate LPA receptors. However, TLC analysis of the radioactively labeled compounds extracted from blood revealed no more than 0.01% of the injected material at the position of the authentic [^{3}H]-OTP standard, indicating that the little amount of radioactivity represents metabolites of the compound. The very low amount of [^{3}H]-OTP found in the blood after oral administration is reinforced by the lack of metabolism by pancreatic lipase and LPP1 present in the intestinal lumen, because these enzymes would produce the neutral oleyl alcohol, which could more effectively be taken up than a charged compound like OTP.

Orally Applied OTP Is Nontoxic in the Effective Dose Range

We tested OTP applied through oral gavage into the stomach of mice at 3, 10, and 30 mg/kg complexed in 1 mmol/L BSA in PBS. Observation of the animals for 1 hour after administration did not show any noticeable change in behavior and motor activity. Monitoring the weight gain curves of the animals showed only a 24-hour transient decrease in weight amounting to a mean of 3 g and only in the 30 mg/kg treatment group, but these animals rebounded by the second day and the median weight of the group was not significantly different from the vehicle-treated controls beyond that up to 5 days, the time the weight of the animals was followed daily. Thus, OTP showed no serious side effects even when administered at a 60-fold concentration (the highest dose tested so far) higher than the 0.5-mg/kg dose, which was highly effective in protecting the life of animals from lethal doses of irradiation (see following text).

OTP Surpasses the Antiapoptotic Activity of LPA in IEC-6 Cells

We previously showed that LPA protects intestinal epithelial cells from apoptosis induced by 4 different mechanisms.12,13,31 We compared the antiapoptotic effect of OTP with that of LPA. Although both OTP and LPA dose-dependently protected IEC-6 cells from gamma irradiation–induced DNA damage, OTP at concentrations greater than 1 μmol/L conferred significantly higher protection (Figure 2*A*). Both OTP and LPA applied at 10 μmol/L significantly protected IEC-6 cells from either topoisomerase inhibitor camptothecin- or the proinflammatory cytokine TNF-α–induced DNA damage as compared with control ($P < .001$), and at this concentration OTP showed stronger antiapoptotic activity than did LPA ($P < .05$; Figure 2*B*). OTP and LPA significantly inhibited caspase-3 and caspase-9 activity induced with gamma irradiation; again, the OTP-induced inhibition was significantly higher than that of LPA ($P < .05$, Figure 2*C*). Furthermore, analysis of caspase-3 activation by Western blotting showed that both OTP and LPA significantly inhibited the conversion of the 32-kilodalton pro-caspase into its active form, and OTP showed significantly higher inhibition compared with LPA (Figure 2*D*; $P < .05$). Lastly, a brief 15-minute OTP treatment inhibited the TNF-α–induced activation of caspase-8 (Figure 2*E*), which provides further support for its effect in reducing apoptosis elicited via the extrinsic pathway. These results together indicate that OTP mimics the antiapoptotic action of LPA in IEC-6 cells that express LPA_1 and LPA_2 receptors.13

The Antiapoptotic Activity of OTP Requires PTX-Sensitive G Protein, Mitogen-Activated Protein Kinase, and PI3K/AKT Signaling

We have previously shown that in IEC-6 cells the antiapoptotic action of LPA requires PTX-sensitive G protein, MEK, and PI3K signaling.13 We found that OTP, just like LPA, activated ERK1/2 and p38 mitogen-activated protein kinase and AKT phosphorylation (Figure 3*A*–*C*). We did not detect c-Jun-N-terminal kinase phosphorylation under identical conditions (data not shown). To evaluate whether these same signaling mechanisms are required for OTP-elicited antiapoptotic activity, we examined these pathways by using pharmacologic inhibitors and exposing these cells to OTP or LPA with or without 25 Gy gamma irradiation. In nonirradiated cells, just like LPA, OTP treatment for 5 minutes induced a significant increase in ERK1/2, p38, and AKT phosphorylation (Figure 3). Blocking of ERK1/2 and AKT activation upstream by the MEK inhibitor PD98059 and PI3K inhibitor LY294002 completely abolished both OTP- and LPA-elicited activation, as well as protection (Figure 3*A, C*, and *D*), indicating that the antiapoptotic activity of OTP required the activation of the ERK1/2 and AKT pathways. Pretreatment of IEC-6 cells with PTX completely abolished LPA-elicited ERK1/2 and AKT activation (Figure 3*A* and *C*). In agreement with the requirement for a PTX-sensitive G protein in the antiapoptotic mechanism, PTX cancelled LPA-elicited protection from gamma irradiation–induced DNA damage. In contrast, although PTX abolished OTP-induced AKT phosphorylation, it only partially attenuated ERK1/2 activation, indicating that OTP-stimulated ERK1/2 activation was mediated through not only PTX-sensitive G proteins. In support of this result, PTX pretreatment only partially reduced OTP-initiated protection, which remained statistically significant following treatment with this toxin ($P < .05$; Figure 3*D*). These results indicate some similarities, as well as differences, between the signaling pathways used by OTP and LPA. Because LPA_1 and LPA_2 are the 2 main EDG family receptors expressed in IEC-6 cells13 and also in the mouse intestine,8,12 we next compared the role of the individual LPA receptors in the LPA-and OTP-elicited antiapoptotic response.

OTP Selectively Protects LPA_2 Transfectants From TNF-α–Induced Apoptosis

RH7777 cells do not endogenously express the EDG family LPA receptor but express low amounts of LPA_5 transcripts.7 When LPA or OTP was applied to wild-type RH7777 cells exposed to TNF-α plus cycloheximide to induce apoptosis, neither compound applied at 10

μmol/L attenuated DNA fragmentation (Figure 4*A*). In contrast, in RH7777 cells individually transfected with LPA_1, LPA_2, or LPA_3, DNA fragmentation was significantly reduced by LPA pretreatment (Figure 4*A*). OTP applied at 10 μmol/L showed no significant antiapoptotic activity in LPA_1 or LPA_3 stable transfectants but evoked highly significant protection in the LPA_2 transfectants, surpassing the effect of that of 10 μmol/L LPA (Figure 3*A*; $P < .001$). It is important to note that OTP and LPA both activate Ca^{2+} transients in LPA_1, LPA_2, or LPA_3 transfectants (Figure 1*C*) but not in wild-type RH7777 cells. Thus, the antiapoptotic effect of OTP is not simply linked to activation of receptor-elicited Ca^{2+} mobilization but to the activation of more complex signals originating from a specific receptor subtype, which is LPA_2. The protective effect of LPA in LPA_1 and LPA_2 transfected RH7777 cells was abolished by PTX and was cancelled by pharmacologic blockade of MEK/ERK1/2 and PI3K/AKT activation, which mirrors our findings in IEC-6 cells (compare Figure 4*B* and Figure 3*D*). Just as in IEC-6 cells, the protective effect of OTP in RH7777 LPA_2 transfectants was only partially PTX sensitive and was completely abolished only by blocking ERK1/2 and PI3K/AKT pathways (Figure 4*B*). These results identify LPA_2 in this model system as the main target of OTP and pinpoint a mechanism that involves MEK/ERK1/2 and PI3K/AKT activation mediated through multiple PTX-insensitive and -sensitive G proteins. LPA_2 is known to be coupled to G_q and it mediates ERK1/2 activation in part,10 a finding consistent with the partial inhibitory effect of PTX on the apoptotic effect found in IEC-6 cells and in LPA_2 transfected RH7777 cells. However, this finding does not explain why OTP, unlike LPA, failed to attenuate apoptosis in LPA_1 or LPA_3 transfected RH7777 cells even though it activated these receptor subtypes indicated by the Ca^{2+} responses (Figure 1*C*).

OTP Attenuates Radiation-Induced Apoptosis in the Intestine

We have previously shown that LPA given orally prevents apoptosis induced by gamma irradiation in the stem cell region of the intestinal crypt.12 Here, we sought to test whether OTP exerted a similar effect and compared its antiapoptotic efficacy with that of LPA by quantifying apoptotic bodies in the jejunal epithelium 4 hours after 15 Gy gamma irradiation (~$LD_{100/10}$). In agreement with our previous report12 using ICR mice, the number of apoptotic bodies in the jejunum of control nonirradiated animals was less than 0.5 per crypt-villus unit (Figure 5*A*). In vehicle-treated (100 μL of 200 μmol/L BSA in PBS) wild-type C57BL/6 mice, the number of apoptotic bodies per crypt-villus unit increased 6-fold 4 hours following gamma irradiation. Oral pretreatment with LPA (2 mg/kg into the stomach 2 hours before irradiation) significantly reduced the number of apoptotic bodies per crypt-villus unit ($P < .01$; Figure 5*A*). Oral OTP pretreatment (same timing and dose as LPA) reduced the number of apoptotic bodies by 50%, which was significantly higher than that elicited by LPA ($P < .05$; Figure 5*A*). Analysis of the distribution of the apoptotic bodies along the crypt-villus unit showed that gamma irradiation resulted in a high frequency of apoptotic cells over the stem cell zone of the crypt, 4–7 cell positions from the base (Figure 5*B*). Both LPA and OTP significantly reduced the number of apoptotic cells over the stem cell zone in the irradiated animals.

Our in vitro data using the RH7777 heterologous overexpression model indicated that OTP elicited its antiapoptotic action through the LPA_2 receptor subtype (Figure 4). To evaluate which LPA receptor mediates the protective effect of OTP in vivo, we performed the same treatments in LPA_1 and LPA_2 KO mice. We detected no difference in the basal count of apoptotic bodies between wild-type C57BL/6 mice and LPA_1 or LPA_2 KO mice on this same genetic background. Surprisingly, gamma irradiation induced a significantly higher rate of apoptosis at the base of the crypt, in LPA_2 KO mice, compared with that in wild-type mice, whereas there was no difference between wild-type and LPA_1 mice (Figure 5*A*). LPA and OTP had the same protective effect in wild-type and LPA_1 mice. In contrast, LPA and

OTP failed to attenuate gamma irradiation–induced apoptosis in LPA_2 KO mice. In wild-type animals, the biggest radiation-induced increase in apoptotic bodies was found in the stem cell region of the crypt (Figure 5*B*). LPA and OTP caused the biggest decrease in the number of apoptotic cells in this region of the crypt, suggesting that the cellular targets of LPA and OTP include the stem cells. Reverse-transcription polymerase chain reaction analysis of the LPA receptors showed that all but LPA_4 transcripts were expressed in the tissue (Figure 5*C*). The LPA_1 and LPA_2 KO animals showed no compensatory change in the expression of the other LPA receptors. Thus, the in vivo data are consistent with our in vitro findings that LPA_2 is required for the antiapoptotic effect of OTP. Nonetheless, these data differ from the in vitro findings in the case of LPA and point to the essential role of LPA_2 in mediating the in vivo antiapoptotic effect of LPA. Furthermore, the increased rate of apoptosis in LPA_2 KO mice suggests that this receptor may play a physiologic role in the radiation sensitivity of the small intestine. These results also point to the fundamentally different role of these 2 LPA receptor subtypes in radiation sensitivity and apoptotic protection.

Next, we sought to obtain direct evidence that LPA and OTP treatments activate the same signal transduction mechanisms we have identified in vitro. First, we examined whether LPA and OTP attenuate the activation of the main executioner, caspase-3, as we have seen in IEC-6 cells in vitro (Figure 1*C*). Jejunum and ileum sections were immunostained with an antibody specific for the activated form of caspase-3, and the number of positive cells was counted in a minimum of 100 crypt-villus units in slides prepared from groups of 4 animals. In the nonirradiated vehicle-treated group, we could not detect caspase-3–positive cells, possibly due to the low amount of antigen present in cells naturally undergoing apoptosis combined with their low incidence in the healthy small intestine. In contrast, in the vehicle-treated irradiated group, caspase-3–positive cells were readily detected. Both LPA and OTP treatments significantly reduced the number of activated caspase-3–positive cells by ~60% (Figure 6*A**; $P < .05$). The inhibition of caspase-3 activation by LPA and OTP was also confirmed in intestinal epithelial lysates by measuring enzymatic activity (Figure 6*B*). These experiments revealed that, in control nonirradiated animals, a low level of caspase-3 substrate cleaving activity is present, which increased 4-fold after 15 Gy gamma irradiation. LPA and OTP reduced caspase-3 activity significantly, although the inhibitory effect of OTP was greater.

Our previous and present in vitro studies using IEC-6 cells and other types of cells[13,31] have established the requirement of ERK1/2 and AKT activation in the anti-apoptotic response to LPA and OTP. We next determined whether these pathways were activated in intestinal cell homogenates prepared from animals that have been treated with the 2 ligands by oral gavage. As shown in Figure 6*C* and *D*, both agents activated ERK1/2 and AKT phosphorylation as early as 30 minutes after administration in nonirradiated animals. However, the effect of OTP was considerably longer lasting in the tissue compared with the effect of LPA, which was absent in the samples collected 60 minutes after administration.

In vitro studies using IEC-6 cells showed that LPA up-regulated the expression of the antiapoptotic Bcl-2 messenger RNA and had no effect on Bcl-X_L, BAD, and Bak messenger RNA abundance determined by real-time polymerase chain reaction.[13] In jejunum homogenates prepared from LPA- and OTP-treated mice 4 hours after irradiation (6 hours after treatment), we could not detect a significant change in Bcl-X_L or Bcl-2 expression (data not shown). However, immunostaining with a Bcl-X_L specific antibody revealed marked increases in LPA- and OTP-treated animals (Figure 7) compared with jejunum and ileum (not shown) from the vehicle-treated animals. OTP treatment caused the most intense immunostaining (Figure 7*C*), although LPA also elicited a substantial increase in the immunoreactivity (Figure 7*B*). When we tested the levels of Bcl-X_L or Bcl-2 protein in

OTP-treated camptothecin-challenged IEC-6 cells, a transient increase in Bcl-X_L but not in Bcl-2 levels was detected (Figure 7*D*). These results taken together establish strong similarities, as well as some differences, between the prosurvival signals elicited by these 2 agents in cultured cells in vitro and the small intestinal tissue in vivo.

OTP and LPA Enhance Intestinal Crypt Survival After Radiation Injury

Gamma irradiation induces apoptosis in crypt cells, which in turn reduces the regenerative or clonogenic potential leading to the disruption of the barrier and absorptive function in the injured gut. We examined the effect of LPA and OTP on crypt survival in irradiated mice using H&E staining 5FdU and BrdU incorporation to monitor regenerating S-phase enterocytes. Irradiation with a dose of 15 Gy caused a 90% reduction in the number of crypts in jejunum in wild-type mice within 4 days (Figure 8 and Figure 9). Oral LPA or OTP pretreatment enhanced intestinal crypt survival in a dose-dependent manner (Figure 8*A*). OTP treatment of mice with doses >0.2 mg/kg significantly enhanced crypt survival, while LPA treatment required a minimum dose of 1.0 mg/kg to cause a significant protection in crypt survival ($P < .05$; Figure 8*A*). OTP at doses >1 mg/kg maintained a significantly greater number of crypts than did LPA ($P < .05$; Figure 8*A*). Following 15 Gy gamma irradiation, oral OTP applied at 2 mg/kg increased the number of surviving crypts in the jejunum from 10 crypts to an average of 27 crypts (Figure 8*A*).

To further validate LPA_2 as the target of the antiapoptotic action of LPA and OTP, we also examined crypt survival in LPA_2 KO mice treated the same way as their wild-type counterparts described previously. In contrast to irradiated wild-type mice, LPA_1 and particularly LPA_2 KO mice showed lower crypt survival. However, in LPA_1 KO mice, LPA and OTP both elicited significantly increased crypt survival, which was not significantly different from that seen in wild-type mice treated in the same manner. LPA_2 KO mice revealed significantly higher radiation sensitivity. Whereas in wild-type mice exposed to a 15-Gy dose the mean crypt survival per circumference was 10, in LPA_2 KO mice it was as little as 1 crypt (Figure 8*B*). Neither LPA nor OTP applied at 2 mg/kg, the highest dose tested, showed any effect in enhancing intestinal crypt survival in the LPA_2 KO mice. This observation extends the increased rate of apoptosis, and the lack of treatment-induced reduction in apoptotic cells observed in the LPA_2 KO mice, lending strong support to the hypothesis that LPA_2 is the molecular target of the radioprotective effect of LPA and OTP.

OTP Reduces Radiation-Induced Death

Although orally applied OTP did not get absorbed into the systemic circulation in an effective concentration but reduced radiation-induced cell death in the small intestine, we reasoned that if administered systemically, it might exert a protective effect on survival. To test this hypothesis, we turned to an intraperitoneal route of administration and monitored 30-day survival as the primary end point following a 9-Gy dose of gamma irradiation, which in our system approximately equals an $LD_{100/30}$ (Figure 10). In the group of mice that received a 0.5-mg/kg dose 30 minutes before irradiation, we observed a 50% survival to the end of the experiment, whereas all animals in the vehicle-treated group died. These results expand the potential usefulness of OTP from the topical protection of the small intestine following an oral route of administration to a radiomitigating agent effectively reducing death caused by the hematopoietic syndrome.

Discussion

The objective of the present study was to evaluate the effect of OTP, a rationally designed, metabolically stabilized LPA mimic, on radiation-induced apoptosis in vitro and in vivo. Our data indicate that OTP is a highly effective antiapoptotic agent that engages prosurvival

pathways similar to those elicited by LPA through the LPA_2 receptor subtype. OTP shares a pharmacologic profile similar to that of LPA in that it activated the 3 EDG family LPA receptors expressed heterologously in RH7777 cells. The rank order of the median effective concentration values of OTP was LPA_2 (90 nmol/L) < LPA_3 < LPA_1 based on Ca^{2+} transients elicited in this heterologous expression system. These values render OTP a considerably weaker ligand of the 3 LPA receptors compared with LPA 18:1. OTP, when compared with LPA in 3 different apoptosis models, which included radiation- and camptothecin-elicited DNA damage–induced and TNF-α/CHX–elicited extrinsic mechanisms, always surpassed the protective effect of LPA. In agreement with the in vitro cellular models of apoptosis, OTP was more effective in reducing the number of apoptotic bodies, caspase-3–positive cells, and caspase-3 activity in C57BL/6 mice exposed to an $LD_{100/15}$ dose of gamma irradiation.

What may account for the higher efficacy of OTP relative to LPA despite its weaker pharmacologic potency? Although we cannot pinpoint a single reason for the increased efficacy of OTP, there are major differences in its metabolic resistance and bioavailability compared with LPA. First, we found that OTP was not cleaved by pancreatic lipase, the major lipase in the intestine. Second, it is not degraded by LPP1, which is the other major mechanism for the inactivation of LPA.51 Third, due to the lack of a glycerol backbone, unlike LPA, OTP cannot be acylated by lysophosphatidate transacetylases. Fourth, likely due to its polar character, OTP does not transverse the cell membrane readily, and we could not detect radioactively labeled OTP in the blood of experimental animals following application via oral gavage. These differences in its metabolism and bioavailability relative to LPA might represent some of the causes for its higher efficacy in the apoptosis assays. The observation that OTP elicited ERK1/2 and AKT phosphorylation with longer duration in the mouse intestinal tissue certainly supports this hypothesis. At the same time, the lack of absorption of [^{3}H]-OTP into the systemic circulation within a 3-hour period, which appears to be the limit for the duration of its protective time window (data not shown), indicates that it exerts its effect topically from within the intestinal lumen without appearing in a pharmacologically and biologically effective concentration in the bloodstream. Radioactively labeled LPA has been shown to be taken up rapidly (within minutes) into cells where it is rapidly dephosphorylated and reacylated52; nevertheless, ~15% remains intact in the cytoplasm up to 30 minutes after extracellular application.53 These differences in bioavailability could, at least in part, explain the differences in the in vivo efficacy of OTP compared with LPA.

Another important difference was that the LPA_2 receptor subtype is sufficient and necessary for the antiapoptotic effect of OTP. In the receptor reconstitution experiments performed in RH7777 cells stably transfected with the individual receptor subtypes, although OTP activated Ca^{2+} transients through each receptor subtype, only cells expressing LPA_2 were protected against apoptosis. In agreement with the role of LPA_2 in this model system, experiments conducted in LPA_2 KO mice confirmed that this receptor was absolutely necessary for the attenuation of apoptosis and increased crypt survival elicited by OTP. A third line of evidence, namely the increased radiation sensitivity of LPA_2 KO gut tissue compared with wild-type animals, suggests that this receptor subtype is uniquely involved in mediating prosurvival signals. Only if we assign the prosurvival function to LPA_2 can it explain the lack of protective effect in response to LPA administration observed in the LPA_2 KO mice, which continue to express LPA_1 and LPA_3.20 Reverse-transcription polymerase chain reaction analysis has identified only the LPA_1 and LPA_2 receptor subtypes in the mouse intestine, as well as in IEC-6 cells used in the present study.8,9 The partial sensitivity of the OTP-elicited anti-apoptotic response to PTX is consistent with the G_q coupling of LPA_2.10 However, LPA also showed antiapoptotic protection in RH7777 cells expressing either LPA_1 or LPA_3 in the TNF-α/CHX-induced apoptosis model. The RH7777 cells

showed extreme resistance to radiation (Deng and Tigyi, unpublished data, September 2004) that precluded studying the radioprotective effect exerted by these receptors in this model. We do not understand the reasons for this difference and can only speculate that either the higher than physiologic level of receptor over-expression or the differences in the protective signaling mechanism between the TNF-α/CHX and the DNA damage–induced mechanisms could be part of the reason. We also found that caspase-8 activity was attenuated by OTP, indicating that LPA receptor signaling affects the upstream part of the extrinsic apoptotic pathway. Whether this inhibition of caspase-8 activation is unique to LPA_2 or also elicited by other receptor subtypes should be evaluated in future experiments. While this unanswered question does not detract from the importance of LPA_2 in the radioprotective mechanisms activated by LPA or OTP and the natural radiation sensitivity of the gut tissue, further experiments will have to be designed to resolve this apparent contradiction. LPA_2 is distinct from the other 2 subtypes in that its C-terminus has been shown to interact with PDZ and LIM domain-containing proteins.[8,54–57] LPA_2 can signal through specific protein-protein interactions in a non–G protein coupled manner and access triple LIM domain-containing proteins, including TRIP6, zyxin, LPP, and Siva-1[54,56,58] (and Lin, personal communication, September 2006). G protein– linked activation of *c-src* by LPA_2 phosphorylates TRIP6, which in turn augments LPA-induced ERK activation,[54] and could lead to increased BAD phosphorylation and inhibition of procaspase-9.[16] The potential interaction of LPA_2 with Siva-1 offers an exciting possibility, because DNA damage–induced activation of Siva-1 scavenges the antiapoptotic Bcl-X_L.[59–61] LPA_2 could capture Siva-1 and enable Bcl-X_L to attenuate apoptosis triggered by DNA damage. Our findings concerning the increased level of Bcl-X_L in IEC-6 cells and OTP-treated gut favor this hypothesis. The PDZ domain-mediated interactions including the PDZ-binding protein NHERF2 provide yet another link with antiapoptotic signaling, because stable knockdown of NHERF2 in CaCo-2 cells has been found to attenuate LPA_2-induced ERK1/2, AKT, and PLCβ activation.[9,55] These potential signaling interactions between LPA_2 and LIM or PDZ domain proteins await further investigation.

Orally administered OTP may offer other uses that reach beyond the protection of the gastrointestinal system. Orally applied OTP is unlikely to be useful for reducing apoptosis in the hematopoietic system, because it does not get absorbed to a biologically effective concentration in the systemic circulation. However, experiments performed with intraperitoneal application of OTP in irradiated C57BL/6 mice caused a significant reduction in lethality mitigating the lethality of the $LD_{100/30}$ dose to equal that of an $LD_{50/30}$ outcome. Thus, the applicability of OTP for systemic treatment of radiation illness should be the focus of the next experiments.

In summary, the present study identifies OTP as an orally active antiapoptotic agent that targets LPA_2 and distinct prosurvival signals coupled to this receptor. The simple chemical nature of OTP, combined with its metabolic resistance, limited systemic bioavailability, and apparently low acute oral toxicity (>10 mg/kg), make this compound a reasonable candidate for treating radiation injury of the gut and warrants further investigation for its potential therapeutic uses.

Acknowledgments

Supported by US Public Health Service grant HL61469 (to G.T.) and RxBio Inc (W.D. and V.G.).

G.T., D.D.M., L.R.J., V.G., and W.D. are stockholders in RxBio Inc.

The authors thank Dr Jerold Chun (Scripps Research Institute, La Jolla, CA) for providing the LPA receptor KO mouse breeders for the study. The intellectual property related to OTP has been licensed to RxBio Inc by the University of Tennessee Research Foundation for commercialization.

Abbreviations used in this paper

BrdU	bromodeoxyuridine
BSA	bovine serum albumin
CHX	cycloheximide
EDG	endothelial differentiation gene
ERK	extracellular signal–regulated kinase
KO	knockout
LPA	lysophosphatidic acid
LPP	lipid phosphate phosphatase
MEK	mitogen-activated protein kinase/extracellular signal–regulated kinase kinase
OTP	octadecenyl thiophosphate
PI3K	phosphoinositide 3-kinase
PTX	pertussis toxin
TLC	thin-layer chromatography
TNF	tumor necrosis factor.

References

1. Potten CS. Radiation, the ideal cytotoxic agent for studying the cell biology of tissues such as the small intestine. Radiat Res. 2004; 161:123–136. [PubMed: 14731078]
2. Tigyi G, Parrill AL. Molecular mechanisms of lysophosphatidic acid action. Prog Lipid Res. 2003; 42:498–526. [PubMed: 14559069]
3. Moolenaar WH, van Meeteren LA, Giepmans BN. The ins and outs of lysophosphatidic acid signaling. Bioessays. 2004; 26:870–881. [PubMed: 15273989]
4. Ishii I, Fukushima N, Ye X, Chun J. Lysophospholipid receptors: signaling and biology. Annu Rev Biochem. 2004; 73:321–354. [PubMed: 15189145]
5. Noguchi K, Ishii S, Shimizu T. Identification of p2y9/GPR23 as a novel G protein-coupled receptor for lysophosphatidic acid, structurally distant from the Edg family. J Biol Chem. 2003; 278:25600–25606. [PubMed: 12724320]
6. Kotarsky K, Boketoft A, Bristulf J, Nilsson NE, Norberg A, Hansson S, Owman C, Sillard R, Leeb-Lundberg LM, Olde B. Lysophosphatidic acid binds to and activates GPR92, a G protein-coupled receptor highly expressed in gastrointestinal lymphocytes. J Pharmacol Exp Ther. 2006; 318:619–628. [PubMed: 16651401]
7. Lee CW, Rivera R, Gardell S, Dubin AE, Chun J. GPR92 as a new G12/13- and Gq-coupled lysophosphatidic acid receptor that increases cAMP, LPA5. J Biol Chem. 2006; 281:23589–23597. [PubMed: 16774927]
8. Li C, Dandridge KS, Di A, Marrs KL, Harris EL, Roy K, Jackson JS, Makarova NV, Fujiwara Y, Farrar PL, Nelson DJ, Tigyi GJ, Naren AP. Lysophosphatidic acid inhibits cholera toxin-induced secretory diarrhea through CFTR-dependent protein interactions. J Exp Med. 2005; 202:975–986. [PubMed: 16203867]
9. Yun CC, Sun H, Wang D, Rusovici R, Castleberry A, Hall RA, Shim H. LPA2 receptor mediates mitogenic signals in human colon cancer cells. Am J Physiol Cell Physiol. 2005; 289:C2–C11. [PubMed: 15728708]
10. Ishii I, Contos JJA, Fukushima N, Chun J. Functional comparisons of the lysophosphatidic acid receptors, LP_{A1}/VZG-1/EDG-2, LP_{A2}/EDG-4, and LP_{A3}/EDG-7 in neuronal cell lines using a retrovirus expression system. Mol Pharmacol. 2000; 58:895–902. [PubMed: 11040035]

11. Yart A, Chap H, Raynal P. Phosphoinositide 3-kinases in lysophosphatidic acid signaling: regulation and cross-talk with the Ras/mitogen-activated protein kinase pathway. Biochim Biophys Acta. 2002; 1582:107–111. [PubMed: 12069817]
12. Deng W, Balazs L, Wang DA, Van Middlesworth L, Tigyi G, Johnson LR. Lysophosphatidic acid protects and rescues intestinal epithelial cells from radiation- and chemotherapy-induced apoptosis. Gastroenterology. 2002; 123:206–216. [PubMed: 12105849]
13. Deng W, Wang DA, Gosmanova E, Johnson LR, Tigyi G. LPA protects intestinal epithelial cells from apoptosis by inhibiting the mitochondrial pathway. Am J Physiol Gastrointest Liver Physiol. 2003; 284:G821–G829. [PubMed: 12684213]
14. Ye X, Ishii I, Kingsbury MA, Chun J. Lysophosphatidic acid as a novel cell survival/apoptotic factor. Biochim Biophys Acta. 2002; 1585:108–113. [PubMed: 12531543]
15. Kang YC, Kim KM, Lee KS, Namkoong S, Lee SJ, Han JA, Jeoung D, Ha KS, Kwon YG, Kim YM. Serum bioactive lysophospholipids prevent TRAIL-induced apoptosis via PI3K/Akt-dependent cFLIP expression and Bad phosphorylation. Cell Death Differ. 2004; 11:1287–1298. [PubMed: 15297884]
16. Fang X, Yu S, Eder A, Mao M, Bast RC Jr, Boyd D, Mills GB. Regulation of BAD phosphorylation at serine 112 by the Rasmitogen-activated protein kinase pathway. Oncogene. 1999; 18:6635–6640. [PubMed: 10597268]
17. Chou CH, Wei LH, Kuo ML, Huang YJ, Lai KP, Chen CA, Hsieh CY. Up-regulation of interleukin-6 in human ovarian cancer cell via a Gi/PI3K–Akt/NF-kappaB pathway by lysophosphatidic acid, an ovarian cancer-activating factor. Carcinogenesis. 2005; 26:45–52. [PubMed: 15471896]
18. Fischer DJ, Liliom K, Guo Z, Nusser N, Virag T, Murakami-Murofushi K, Kobayashi S, Erickson JR, Sun G, Miller DD, Tigyi G. Naturally occurring analogs of lysophosphatidic acid elicit different cellular responses through selective activation of multiple receptor subtypes. Mol Pharmacol. 1998; 54:979–988. [PubMed: 9855625]
19. Contos JJA, Fukushima N, Weiner JA, Kaushal D, Chun J. Requirement for the lp_{A1} lysophosphatidic acid receptor gene in normal suckling behavior. Proc Natl Acad Sci U S A. 2000; 97:13384–13389. [PubMed: 11087877]
20. Contos JJ, Ishii I, Fukushima N, Kingsbury MA, Ye X, Kawamura S, Brown JH, Chun J. Characterization of lpa(2) (Edg4) and lpa(1)/ lpa(2) (Edg2/Edg4) lysophosphatidic acid receptor knockout mice: signaling deficits without obvious phenotypic abnormality attributable to lpa(2). Mol Cell Biol. 20002; 22:6921–6929. [PubMed: 12215548]
21. Ye X, Hama K, Contos JJ, Anliker B, Inoue A, Skinner MK, Suzuki H, Amano T, Kennedy G, Arai H, Aoki J, Chun J. LPA3-mediated lysophosphatidic acid signalling in embryo implantation and spacing. Nature. 2005; 435:104–108. [PubMed: 15875025]
22. Chevreau N, Funk-Archuleta M. Effect of enteral formulas on methotrexate toxicity. Nutr Cancer. 1995; 23:185–204. [PubMed: 7644387]
23. Funk-Archuleta MA, Foehr MW, Tomei LD, Hennebold KL, Bathurst IC. A soy-derived antiapoptotic fraction decreases meth-otrexate toxicity in the gastrointestinal tract of the rat. Nutr Cancer. 1997; 29:217–221. [PubMed: 9457742]
24. Logvinova AV, Foehr MW, Pemberton PA, Khazalpour KM, Funk-Archuleta MA, Bathurst IC, Tomei LD. Soy-derived antiapoptotic fractions protect gastrointestinal epithelium from damage caused by methotrexate treatment in the rat. Nutr Cancer. 1999; 33:33–39. [PubMed: 10227041]
25. Tokumura A, Fukuzawa K, Akamatsu Y, Yamada S, Suzuki T, Tsukatani H. Identification of vasopressor phospholipid in crude soybean lecithin. Lipids. 1978; 13:468–472. [PubMed: 567731]
26. Sturm A, Dignass AU. Modulation of gastrointestinal wound repair and inflammation by phospholipids. Biochim Biophys Acta. 2002; 1582:282–288. [PubMed: 12069839]
27. Sano T, Baker D, Virag T, Wada A, Yatomi Y, Kobayashi T, Igarashi Y, Tigyi G. Multiple mechanisms linked to platelet activation result in lysophosphatidic acid and sphingosine 1-phosphate generation in blood. J Biol Chem. 2002; 277:21197–21206. [PubMed: 11929870]
28. Hines OJ, Ryder N, Chu J, McFadden D. Lysophosphatidic acid stimulates intestinal restitution via cytoskeletal activation and remodeling. J Surg Res. 2000; 92:23–28. [PubMed: 10864477]

29. Hall PA, Coates PJ, Ansari B, Hopwood D. Regulation of cell number in the mammalian gastrointestinal tract: the importance of apoptosis. J Cell Sci. 1994; 107:3569–3577. [PubMed: 7706406]
30. Pritchard DM, Watson AJ. Apoptosis and gastrointestinal pharmacology. Pharmacol Ther. 1996; 72:149–169. [PubMed: 8981574]
31. Deng W, Poppleton H, Yasuda S, Makarova N, Shinozuka Y, Wang DA, Johnson LR, Patel TB, Tigyi G. Optimal lysophosphatidic acid-induced DNA synthesis and cell migration but not survival require intact autophosphorylation sites of the epidermal growth factor receptor. J Biol Chem. 2004; 279:47871–47880. [PubMed: 15364923]
32. Parrill AL, Wang D, Bautista DL, Van Brocklyn JR, Lorincz Z, Fischer DJ, Baker DL, Liliom K, Spiegel S, Tigyi G. Identification of Edg1 receptor residues that recognize sphingosine 1-phosphate. J Biol Chem. 2000; 275:39379–39384. [PubMed: 10982820]
33. Wang D, Lorincz Z, Bautista DL, Liliom K, Tigyi G, Parrill AL. A single amino acid determines ligand specificity of the $S1P_1$ (EDG1) and LPA_1 (EDG2) phospholipid growth factor receptors. J Biol Chem. 2001; 276:49213–49220. [PubMed: 11604399]
34. Sardar VM, Bautista DL, Fischer DJ, Yokoyama K, Nusser N, Virag T, Wang DA, Baker DL, Tigyi G, Parrill AL. Molecular basis for lysophosphatidic acid receptor antagonist selectivity. Biochim Biophys Acta. 2002; 1582:309–317. [PubMed: 12069842]
35. Parrill AL, Sardar VM, Yuan H. Sphingosine 1-phosphate and lysophosphatidic acid receptors: agonist and antagonist binding and progress toward development of receptor-specific ligands. Semin Cell Dev Biol. 2004; 15:467–476. [PubMed: 15271292]
36. Fujiwara Y, Sardar V, Tokumura A, Baker DL, Murakami-Murofushi K, Parrill AL, Tigyi G. Identification of residues responsible for ligand recognition and regioisomeric selectivity of LPA receptors expressed in mammalian cells. J Biol Chem. 2005; 280:35038–35050. [PubMed: 16115890]
37. Inagaki Y, Pham TT, Fujiwara Y, Kohno T, Osborne DA, Igarashi Y, Tigyi G, Parrill AL. Sphingosine 1-phosphate analogue recognition and selectivity at S1P4 within the endothelial differentiation gene family of receptors. Biochem J. 2005; 389:187–195. [PubMed: 15733055]
38. Jo E, Sanna MG, Gonzalez-Cabrera PJ, Thangada S, Tigyi G, Osborne DA, Hla T, Parrill AL, Rosen H. S1P1-selective in vivo-active agonists from high-throughput screening: off-the-shelf chemical probes of receptor interactions, signaling, and fate. Chem Biol. 2005; 12:703–715. [PubMed: 15975516]
39. Virag T, Elrod DB, Liliom K, Sardar VM, Parrill AL, Yokoyama K, Durgam G, Deng W, Miller DD, Tigyi G. Fatty alcohol phosphates are subtype-selective agonists and antagonists of LPA receptors. Mol Pharmacol. 2003; 63:1032–1042. [PubMed: 12695531]
40. Durgam GG, Virag T, Walker MD, Tsukahara R, Yasuda S, Liliom K, van Meeteren LA, Moolenaar WH, Wilke N, Siess W, Tigyi G, Miller DD. Synthesis, structure-activity relationships, and biological evaluation of fatty alcohol phosphates as lysophosphatidic acid receptor ligands, activators of PPARgamma, and inhibitors of autotaxin. J Med Chem. 2005; 48:4919–4930. [PubMed: 16033271]
41. MOE. Montreal: Chemical Computing Group. 2002
42. Halgren TA. Merck molecular force field. I. Basis, form, scope, parameterization, and performance of MMFF94*. J Comp Chem. 1996; 17:490–519.
43. Morris GM, Goodsell DS, Halliday RS, Huey R, Hart WE, Belew RK, Olson AJ. Automated docking using a Lamarckian genetic algorithm and an empirical binding free energy function. J Comput Chem. 1998; 19:1639–1662.
44. Ballesteros, JA.; Weinstein, H. Methods in neurosciences. Conn, PM.; Sealfon, SC., editors. San Diego: Academic; 1995. p. 366-428.Chapter 19
45. Kates, M. Techniques of lipidology. Amsterdam: Elsevier; 1988.
46. Yue J, Yokoyama K, Balazs L, Baker DL, Smalley D, Pilquil C, Brindley DN, Tigyi G. Mice with transgenic overexpression of lipid phosphate phosphatase-1 display multiple organotypic deficits without alteration in circulating lysophosphatidate level. Cell Signal. 2004; 16:385–399. [PubMed: 14687668]

47. Fischer DJ, Nusser N, Virag T, Yokoyama K, Wang D, Baker DL, Bautista D, Parrill AL, Tigyi G. Short-chain phosphatidates are subtype-selective antagonists of lysophosphatidic acid receptors. Mol Pharmacol. 2001; 60:776–784. [PubMed: 11562440]
48. Balazs L, Okolicany J, Ferrebee M, Tolley B, Tigyi G. Topical application of the phospholipid growth factor lysophosphatidic acid promotes wound healing in vivo. Am J Physiol Regul Integr Comp Physiol. 2001; 280:R466–R472. [PubMed: 11208576]
49. Steiner T. The hydrogen bond in the solid state. Angew Chem Int Ed. 2002; 41:48–76.
50. Ohta H, Sato K, Murata N, Damirin A, Malchinkhuu E, Kon J, Kimura T, Tobo M, Yamazaki Y, Watanabe T, Yagi M, Sato M, Suzuki R, Murooka H, Sakai T, Nishitoba T, Im DS, Nochi H, Tamoto K, Tomura H, Okajima F. Ki16425, a subtype-selective antagonist for EDG-family lysophosphatidic acid receptors. Mol Pharmacol. 2003; 64:994–1005. [PubMed: 14500756]
51. Brindley DN, English D, Pilquil C, Buri K, Ling ZC. Lipid phosphate phosphatases regulate signal transduction through glycerolipids and sphingolipids. Biochim Biophys Acta. 2002; 1582:33–44. [PubMed: 12069808]
52. van der Bend RL, de Widt J, van Corven EJ, Moolenaar WH, van Blitterswijk WJ. Metabolic conversion of the biologically active phospholipid, lysophosphatidic acid, in fibroblasts. Biochim Biophys Acta. 1992; 1125:110–112. [PubMed: 1567902]
53. Tokumura A, Tsutsumi T, Tsukatani H. Transbilayer movement and metabolic fate of ether-linked phosphatidic acid (1-O-Octadecyl-2-acetyl-sn-glycerol 3-phosphate) in guinea pig peritoneal polymorphonuclear leukocytes. J Biol Chem. 1992; 267:7275–7283. [PubMed: 1559972]
54. Lai YJ, Chen CS, Lin WC, Lin FT. c-Src-mediated phosphorylation of TRIP6 regulates its function in lysophosphatidic acid-induced cell migration. Mol Cell Biol. 2005; 25:5859–5868. [PubMed: 15988003]
55. Oh YS, Jo NW, Choi JW, Kim HS, Seo SW, Kang KO, Hwang JI, Heo K, Kim SH, Kim YH, Kim IH, Kim JH, Banno Y, Ryu SH, Suh PG. NHERF2 specifically interacts with LPA2 receptor and defines the specificity and efficiency of receptor-mediated phospholipase C-beta3 activation. Mol Cell Biol. 2004; 24:5069–5079. [PubMed: 15143197]
56. Xu J, Lai YJ, Lin WC, Lin FT. TRIP6 enhances lysophosphatidic acid-induced cell migration by interacting with the lysophosphatidic acid 2 receptor. J Biol Chem. 2004; 279:10459–10468. [PubMed: 14688263]
57. Yamada T, Ohoka Y, Kogo M, Inagaki S. Physical and functional interactions of the lysophosphatidic acid receptors with PDZ domain-containing Rho guanine nucleotide exchange factors (RhoGEFs). J Biol Chem. 2005; 280:19358–19363. [PubMed: 15755723]
58. Takizawa N, Smith TC, Nebl T, Crowley JL, Palmieri SJ, Lifshitz LM, Ehrhardt AG, Hoffman LM, Beckerle MC, Luna EJ. Supervillin modulation of focal adhesions involving TRIP6/ZRP-1. J Cell Biol. 2006; 174:447–458. [PubMed: 16880273]
59. Chu F, Borthakur A, Sun X, Barkinge J, Gudi R, Hawkins S, Prasad KV. The Siva-1 putative amphipathic helical region (SAH) is sufficient to bind to BCL-XL and sensitize cells to UV radiation induced apoptosis. Apoptosis. 2004; 9:83–95. [PubMed: 14739602]
60. Gudi R, Barkinge J, Hawkins S, Chu F, Manicassamy S, Sun Z, Duke-Cohan JS, Prasad KV. Siva-1 negatively regulates NF-kappaB activity: effect on T-cell receptor-mediated activation-induced cell death (AICD). Oncogene. 2006; 25:3458–3462. [PubMed: 16491128]
61. Xue L, Chu F, Cheng Y, Sun X, Borthakur A, Ramarao M, Pandey P, Wu M, Schlossman SF, Prasad KV. Siva-1 binds to and inhibits BCL-X(L)-mediated protection against UV radiation-induced apoptosis. Proc Natl Acad Sci U S A. 2002; 99:6925–6930. [PubMed: 12011449]

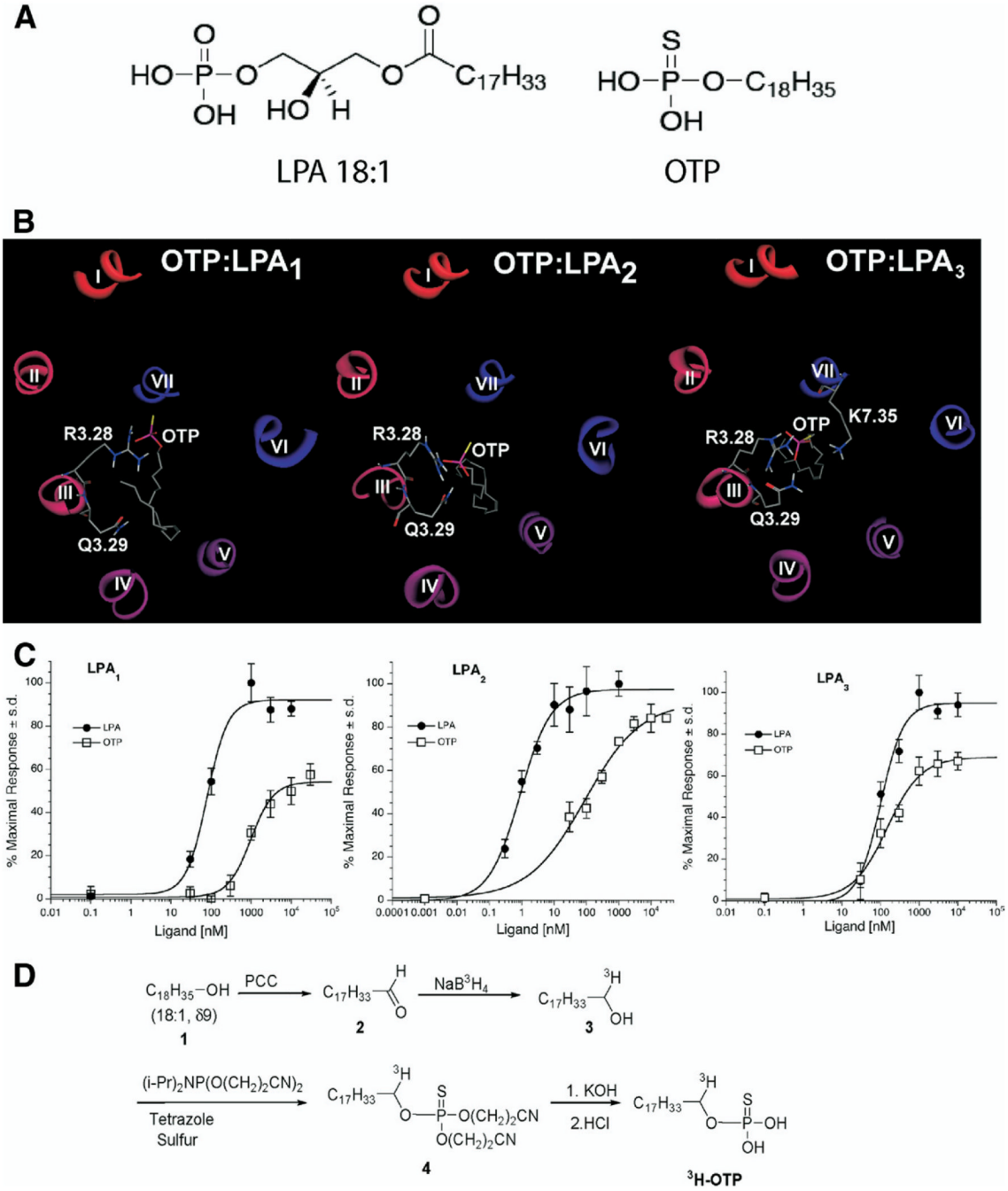

Figure 1.

(*A*) Chemical structures of LPA and OTP. (*B*) Molecular models of OTP docked into the ligand-binding pocket of LPA receptors. (*C*) Ca^{2+} transients elicited by OTP and LPA in RH7777 cells stably expressing the individual EDG family LPA receptors. Wild-type RH7777 cells show no Ca^{2+} transients in response to LPA up to concentrations as high as 30 μmol/L (data not shown). (*D*) Synthesis of ^{3}H-labeled OTP (see Materials and Methods for details).

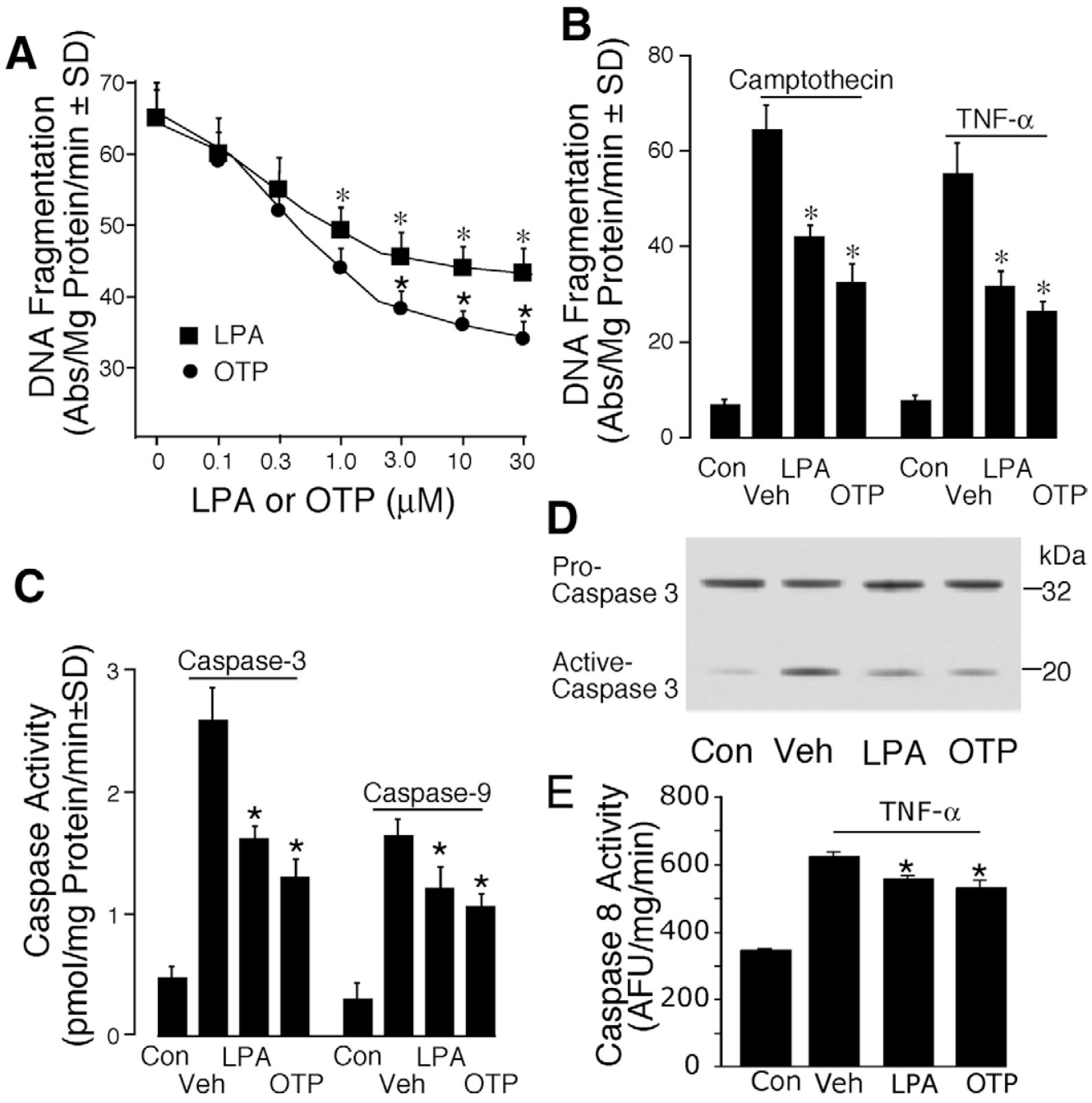

Figure 2.

OTP is more effective in reducing apoptosis than is LPA in IEC-6 cells. (*A*) IEC-6 cells were washed twice and starved in serum-free Dulbecco's modified Eagle medium overnight. OTP (*circles*) or LPA (*squares*), ranging from 0 to 30 μmol/L, was applied 15 minutes before 25 Gy gamma irradiation. DNA fragmentation was evaluated 18 hours postirradiation as described in Materials and Methods. (*B*) IEC-6 cells were treated with either 10 μmol/L OTP or LPA before exposure to 20 μmol/L camptothecin or 20 ng/mL TNF-α plus 10 μg/mL cycloheximide. DNA fragmentation was evaluated 6 hours later. Con, nontreated control cells; Veh, cells treated with vehicle (10 μmol/L BSA). (*C*) Vehicle, 10 μmol/L OTP or LPA, was applied to IEC-6 cells 15 minutes before 25 Gy gamma irradiation. Caspase-3 and

caspase-9 activities were measured 18 hours postirradiation by enzyme-linked immunosorbent assay. (*D*) Western blot analysis of caspase-3 activation in LPA- and OTP-treated (10 μmol/L each) EC-6 cells 15 minutes before 25 Gy gamma irradiation. A total of 20 μg cytosolic protein was loaded for each lane. (*E*) A 15-minute OTP or LPA pretreatment inhibits 20 ng/mL TNF-α plus 10 μg/mL cycloheximide-induced caspase-8 activity. **P*< .01 compared with the appropriate control group. Data shown are means ± SD of at least 3 experiments.

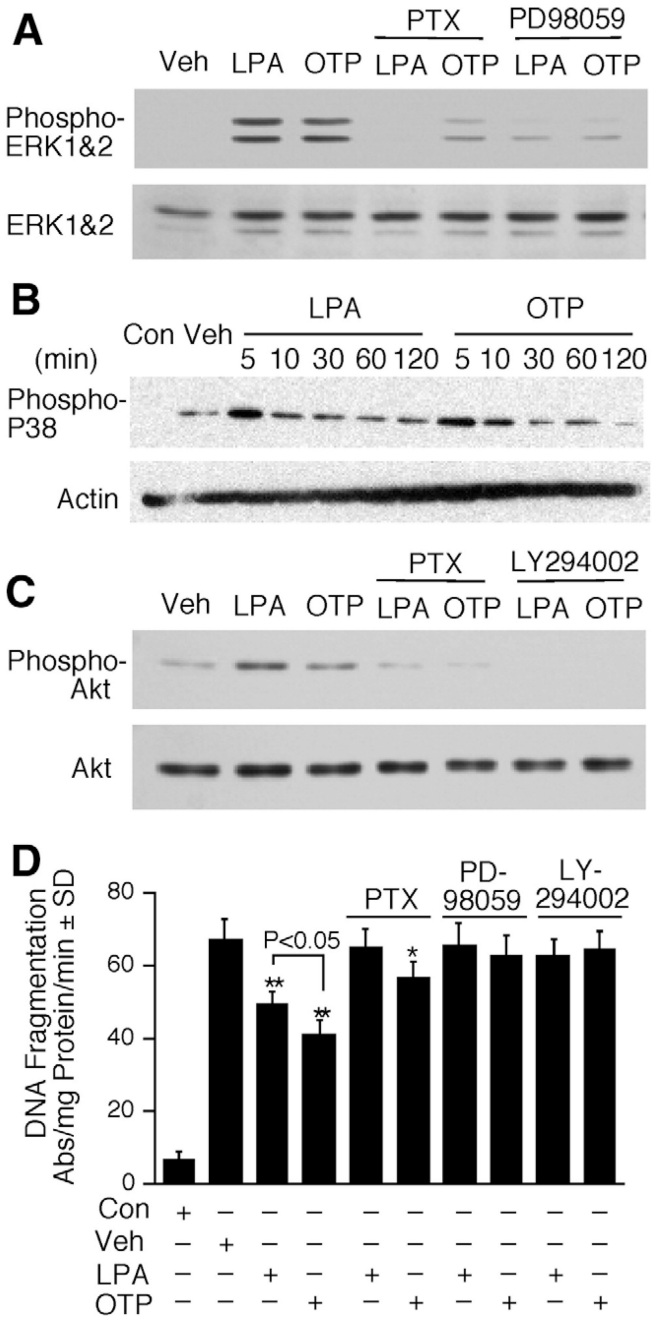

Figure 3.

Activation of prosurvival signaling pathways by LPA and OTP in IEC-6 cells. IEC-6 cells were pretreated with PTX (50 ng/mL) overnight, PD98059 (20 μmol/L) for 1 hour, or LY294002 (10 μmol/L) for 30 minutes, followed by the addition of 10 μmol/L OTP or LPA. Activation of (*A*) ERK1/2, (*B*) P38 mitogen-activated protein kinase, and (*C*) PKB/ AKT was evaluated by Western blot after treatment with 10 μmol/L OTP or LPA. A total of 20 μg lysate protein was loaded for each lane. (*D*) IEC-6 cells were exposed to 25 Gy gamma irradiation 15 minutes after OTP or LPA treatment (10 μmol/L). DNA fragmentation was evaluated 18 hours postirradiation. **P*< .05 compared with irradiation alone. ***P*< .01 compared with irradiation alone. Data shown are means ± SD of at least 3 experiments.

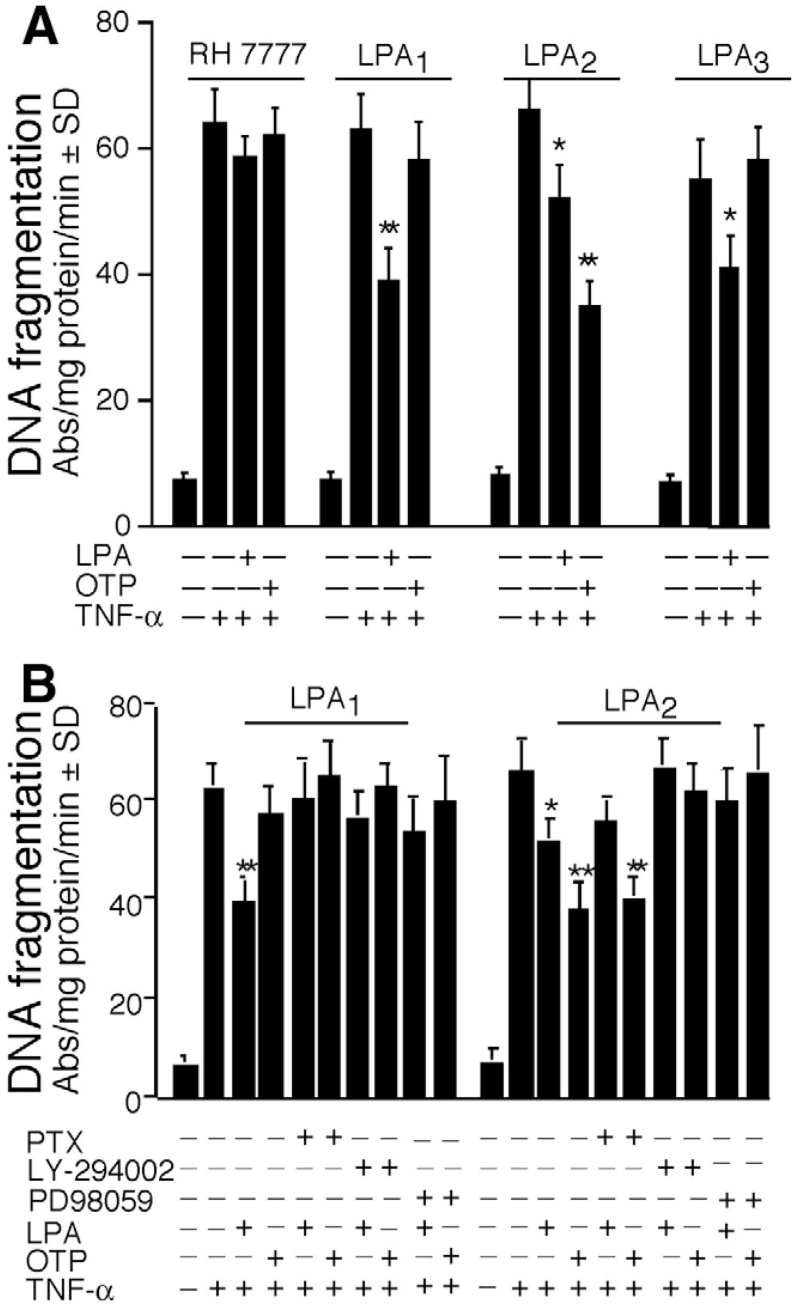

Figure 4.

OTP selectively protects LPA_2 transfectants against TNF-α/CHX–induced apoptosis. (*A*) RH7777 cells were transfected with empty pCDNA3.1 vector or LPA_1, LPA_2, or LPA_3 and preincubated with 10 μmol/LOTP or LPA for 15 minutes, followed by TNF-α (20 ng/mL) plus CHX (10 μg/mL) exposure to induce apoptosis. Note that whereas LPA reduced TNF-α/CHX–induced DNA fragmentation in all 3 transfectants, OTP was effective only in LPA_2 cells. Both ligands elicited Ca^{2+} transients in these same cell lines (see Figure 1*C*). (*B*) LPA_1 and LPA_2 transfectants were pretreated with PTX overnight (50 ng/mL), the MEK inhibitor PD98059 (20 μmol/L) for 1 hour, or the PI3K inhibitor LY294002 (10 μmol/L) for 30 minutes, followed by the addition of 10 μmol/L OTP or LPA for 15 minutes and

challenged with TNF-α (20 ng/mL) plus CHX (10 μg/mL). DNA fragmentation was evaluated 6 hours after addition of TNF-α/CHX. The reduction in DNA fragmentation was partially sensitive to PTX in LPA_2 cells and was abolished in LPA_1 cells. **P*< .05, ***P*< .001 compared with TNF-α/CHX alone. Data shown are means ± SD of 3 experiments.

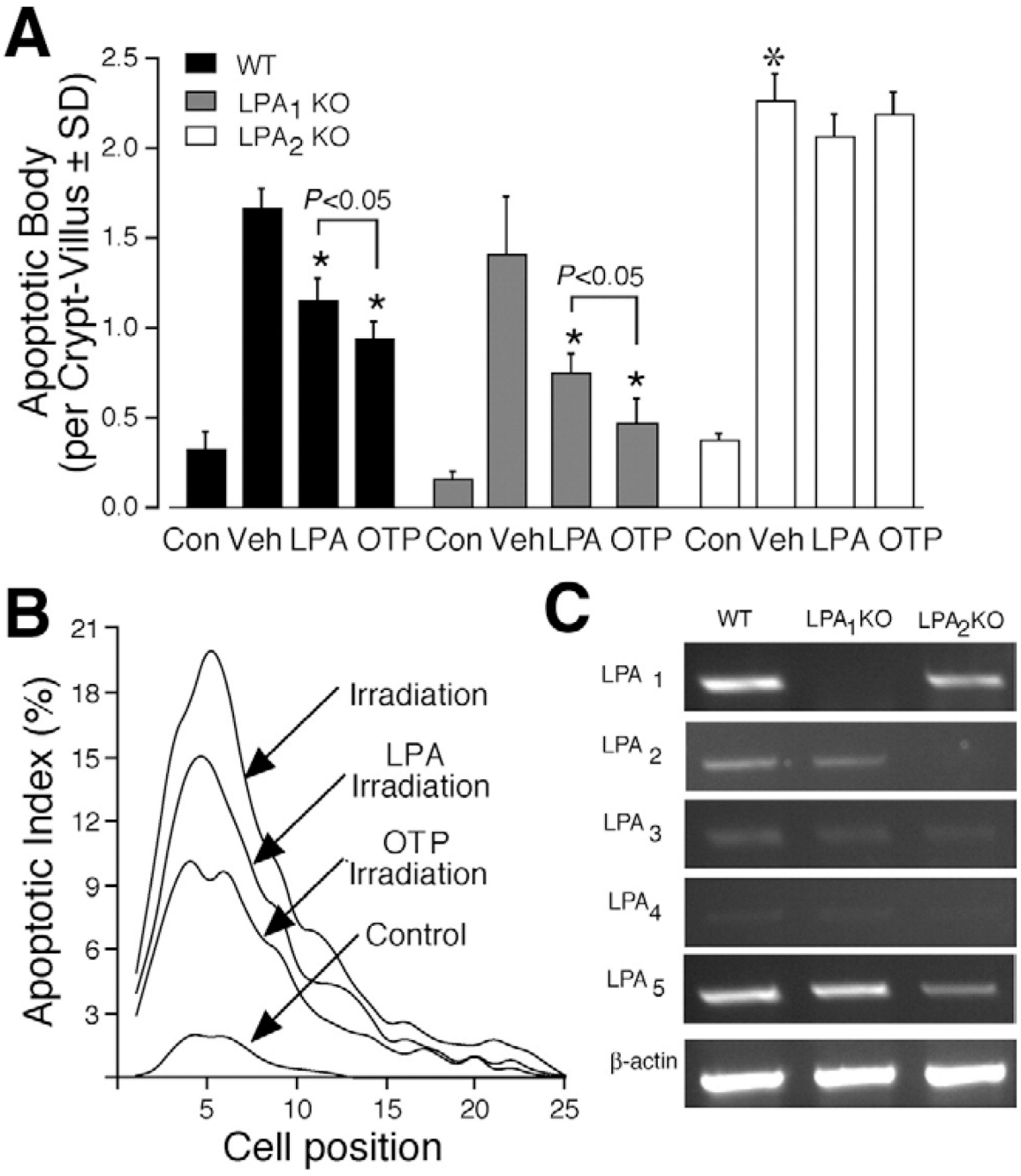

Figure 5.

OTP inhibits apoptosis in small intestinal epithelium of mice following gamma irradiation. Wild-type C57BL/6 (*closedbars*) and LPA_1 (*gray bars*) or LPA_2 KO mice (*open bars*) were given vehicle orally (100 μL of 200 μmol/L BSA control), LPA (2 mg/kg), or OTP (2 mg/kg) 2 hours before subjecting them to 15 Gy whole body gamma irradiation. Animals were killed 4 hours after irradiation to evaluate apoptosis in the small intestine by H&E staining. (*A*) The mean number of apoptotic cells per crypt-villus unit. Both LPA and OTP caused a statistically significant decrease in the number of apoptotic bodies compared with the vehicle-treated animal group ($P < .01$). Furthermore, OTP was significantly more effective than LPA (*$P < .05$). The number of apoptotic bodies was significantly higher in the LPA_2

KO mice compared with wild-type or LPA_1 mice (*P< .01). (*B*) Correlation between apoptotic cell index (percentage of apoptotic cells at a given cell position) and their position along the crypt-villus axis. Cells 1–2 are Paneth cells in the graph. n = 6 animals in each group, and a minimum of 100 crypt-villus units was scored in each group. (*C*) Reverse-transcription polymerase chain reaction analysis of LPA G protein–coupled receptors in jejunum isolated from wild-type, $LPA_1^{-/-}$, and $LPA_2^{-/-}$ mice.

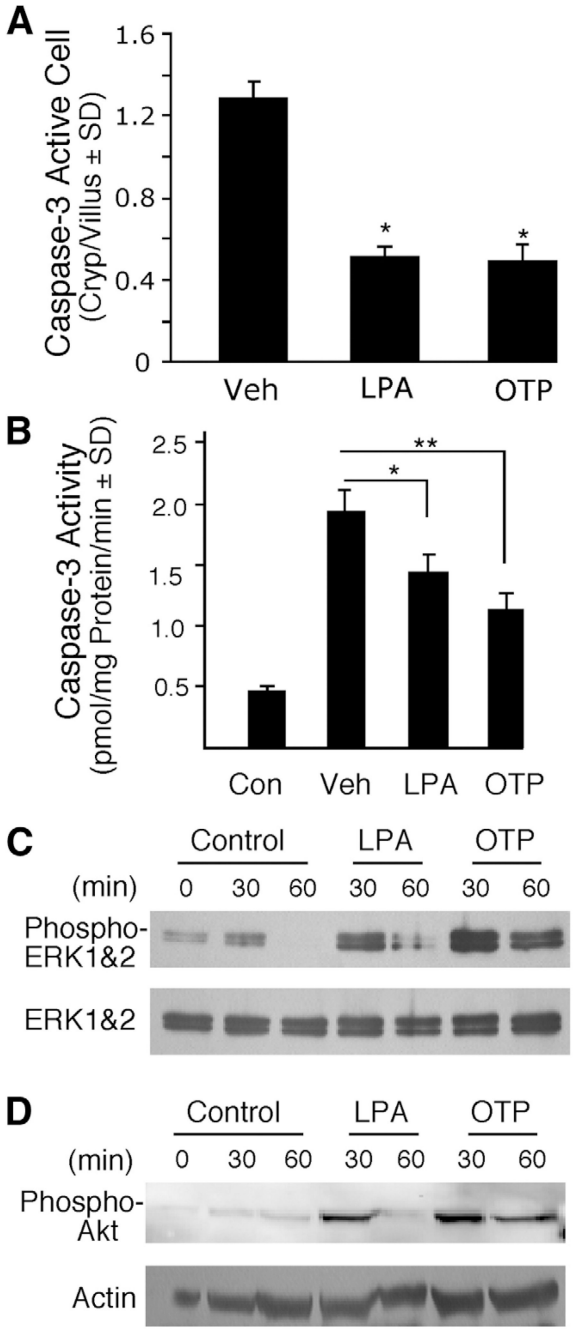

Figure 6.

OTP and LPA reduced caspase-3 activation and activated prosurvival pathways in vivo. C57BL/6 mice were pretreated with 2 mg/kg LPA or OTP for 2 hours and subjected to 15 Gy radiation exposure. Mice were killed 4 hours after radiation. (*A*) Quantification of active caspase-3 immunoreactive cells. Paraffin-embedded jejunum sections from animals treated with radiation and pretreated with either LPA or OTP were stained with a rabbit polyclonal active caspase-3 antibody and fluorescein-labeled secondary antibody using indirect immunofluorescence as described in Materials and Methods, and the sections were counterstained with 4′,6-diamidino-2-phenylindole (DAPI). Active caspase-3 immunoreactive cells were counted in a minimum of 100 crypt-villus units in groups of 4

animals in the groups. Both agents significantly reduced the number of activated caspase-3–positive cells (*P< .05) when compared with vehicle-treated controls. (*B*) Caspase-3 activity was determined in epithelial cell lysates prepared from the same animals whose jejunum segments were used for activated caspase-3 immunostaining in *A*. LPA and OTP both significantly reduced caspase-3 activity in the tissue lysates, a finding in agreement with the reduced number of active caspase-3 cells. (*P< .05, **P< .01) (*C* and *D*) Jejunum tissue from mice orally treated with vehicle, 2 mg/kg LPA, or OTP for the indicated times was homogenized and lysates were analyzed using Western blotting with (*C*) anti–phospho-ERK1/2 or (*D*) anti–phospho-AKT antibodies and appropriate antibodies to the non-phosphorylated forms of the kinases to monitor equal loading. Note that the activation of both kinases was more robust and longer lasting for OTP compared with LPA.

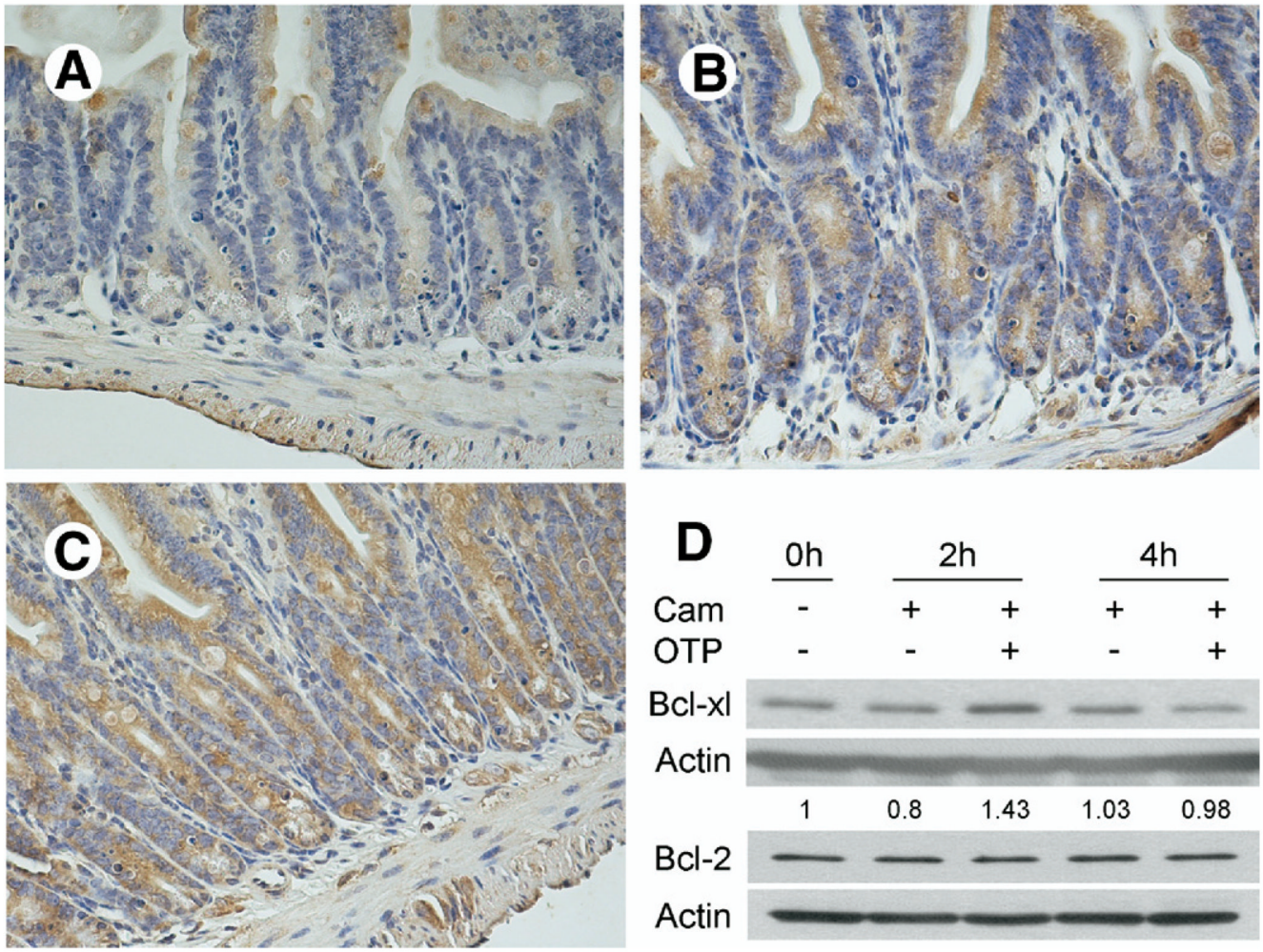

Figure 7.

Immunohistochemical localization of antiapoptotic Bcl-X_L protein in vehicle- (200 μmol/L BSA), LPA-, and OTP-pretreated (2 mg/kg each) irradiated small intestinal sections of C57BL/6 mice. Sections of (*A*) vehicle-treated mice showed less Bcl-X_L expression compared with sections obtained from mice treated with (*B*) LPA or (*C*) OTP. *Calibration bar* = 200 μm. The patterns shown are representative to sections obtained from all mice in the corresponding group of 4 mice per treatment. (*D*) OTP increases the cytoplasmic level of Bcl-X_L but not Bcl-2 in camptothecin-treated EC-6 cells. After overnight serum starvation, IEC-6 cells were pretreated with 10 μmol/L OTP or vehicle for 1 hour before challenge with 20 μmol/L camptothecin (Cam). A 20 μg cytoplasmic protein was loaded for each lane and blotted with anti–Bcl-X_L or anti–Bcl-2 antibodies as described in Materials and Methods. Note that OTP increased the amount of Bcl-X_L but not of Bcl-2 that peaked at 2 hours after camptothecin and decreased to control level by 4 hours.

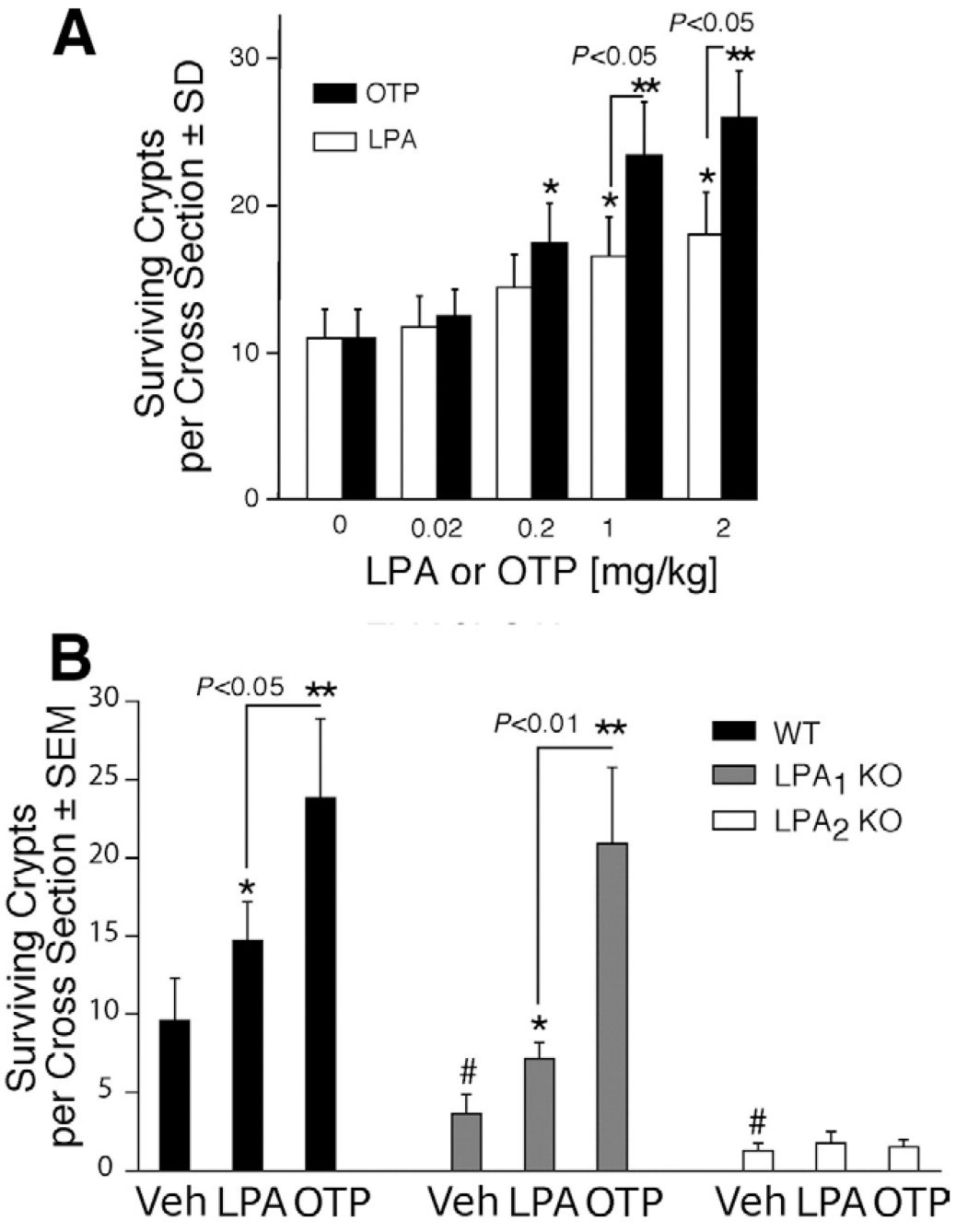

Figure 8.

Clonogenic regeneration assays reveal increased intestinal crypt survival in OTP- and LPA-treated mice following irradiation. (*A*) Wild-type C57BL/6 mice were given either vehicle (BSA 200 μmol/ L), LPA, or OTP (0–2 mg/kg) orally 2 hours before being subjected to 15 Gy whole body gamma irradiation. (*B*) Wild-type C57BL/6 (*closedbars*), LPA1 KO (*gray bars*), or LPA_2 KO mice (*open bars*) were orally given vehicle, LPA, or OTP, 2 mg/kg, 2 hours before 15 Gy gamma irradiation, and the animals were killed 4 days after irradiation. Crypt survival was evaluated by H&E staining combined with BrdU immunostaining. n = 6 in each group. Data are expressed as means ± SD of surviving crypts per cross section. The level of significance based on Student *t* test was **P*< .05 or ***P*< .01 between the designated

groups and was $^{\#}P < .01$ compared with irradiation alone and between the mean crypt survival in wild-type and LPA_1 and LPA_2 KO mice.

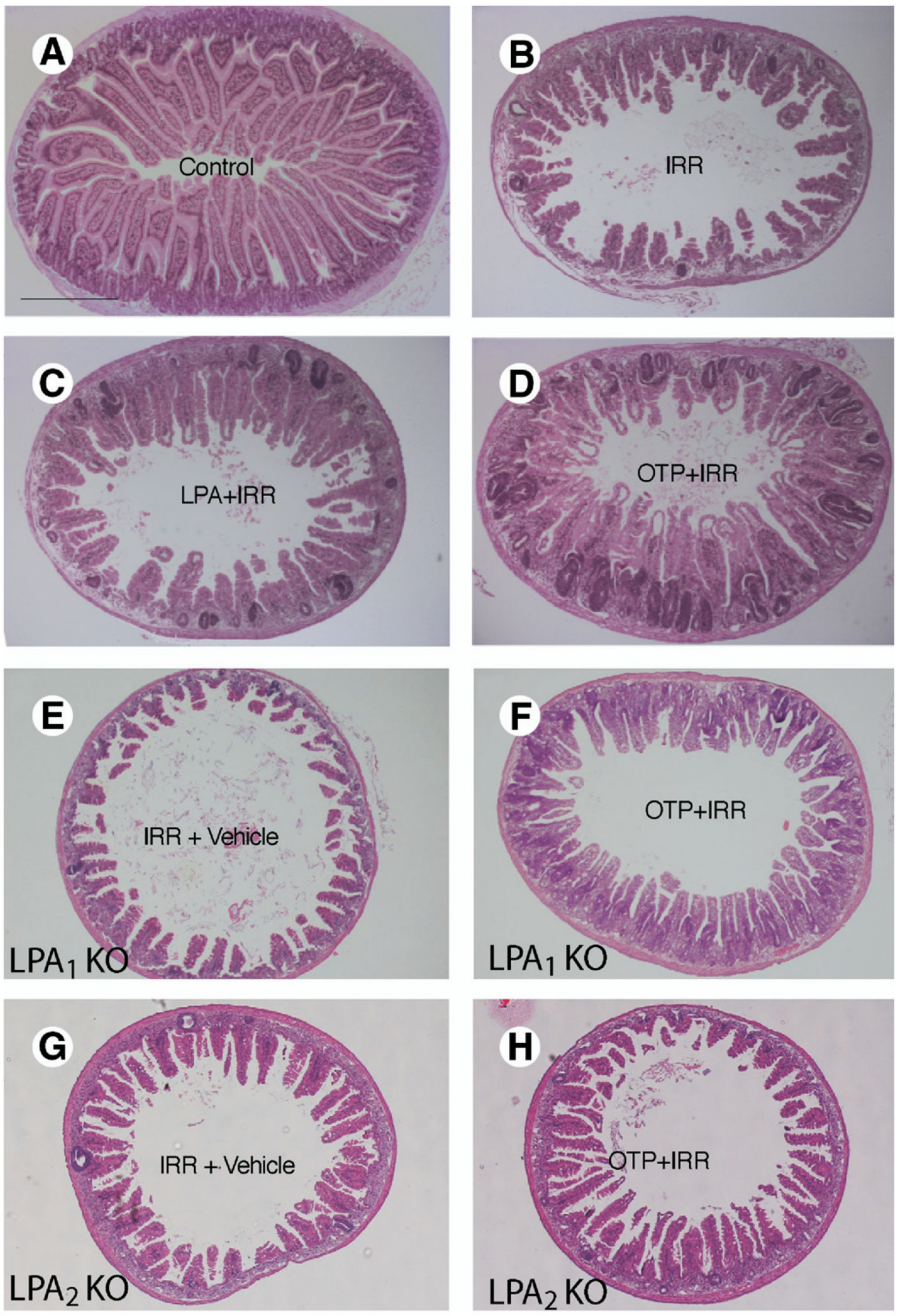

Figure 9.

Representative H&E-stained gut cross sections from (*A*) nonirradiated control, (*B*) irradiated vehicle-treated, (*C*) LPA-treated (2 mg/kg), and (*D*) OTP-treated wild-type (2 mg/kg) mice, (*E* and *G*) vehicle-treated LPA_1 and LPA_2 KO mice, and OTP-treated (2 mg/kg) (*F*) LPA_1 KO and (*H*) LPA_2 KO mice taken 4 days after irradiation. *Calibration bar* = ~500 μm.

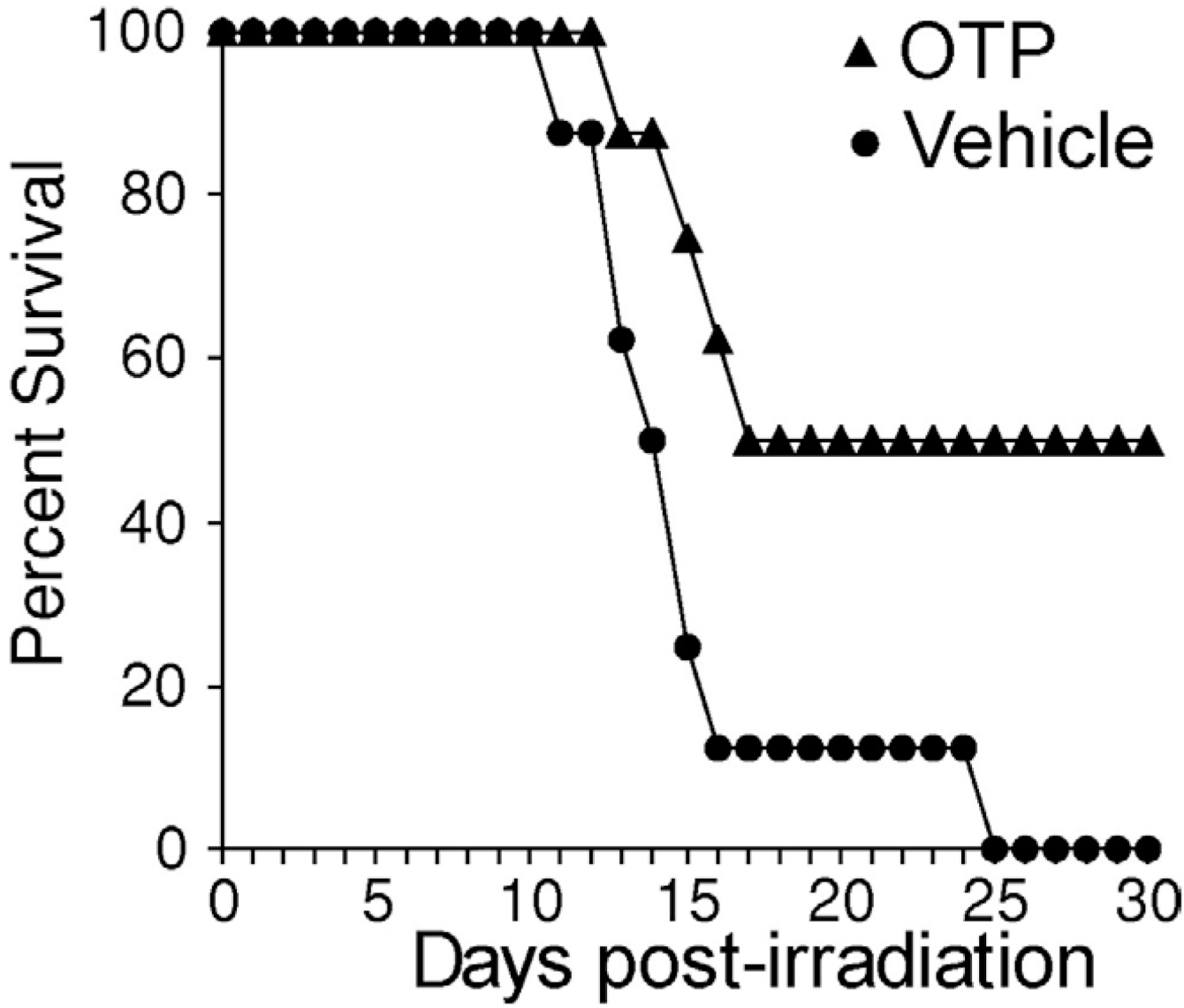

Figure 10.
OTP administered intraperitoneally 30 minutes before irradiation with a 9-Gy ($LD_{100/30}$) dose increased 30-day survival over vehicle-treated controls.